uOttawa

L'Université canadienne
Canada's university

FACULTÉ DES ÉTUDES SUPÉRIEURES ET POSTOCTORALES

uOttawa

L'Université canadienne
Canada's university

FACULTY OF GRADUATE AND POSDOCTORAL STUDIES

Cristina Basile

AUTEUR DE LA THÈSE / AUTHOR OF THESIS

M.Sc. (Cellular and Molecular Medicine)

GRADE / DEGREE

Department of Cellular and Molecular Medicine

FACULTÉ, ÉCOLE, DÉPARTEMENT / FACULTY, SCHOOL, DEPARTMENT

Acute Injury of Hippocampal Dentate Gyrus and Hilus by Elevated External Potassium

TITRE DE LA THÈSE / TITLE OF THESIS

Dr. B. Hu

DIRECTEUR (DIRECTRICE) DE LA THÈSE / THESIS SUPERVISOR

CO-DIRECTEUR (CO-DIRECTRICE) DE LA THÈSE / THESIS CO-SUPERVISOR

EXAMINATEURS (EXAMINATRICES) DE LA THÈSE / THESIS EXAMINERS

Dr. D. McIntyre

Dr. S. Bennett

Gary W. Slater

Le Doyen de la Faculté des études supérieures et postdoctorales / Dean of the Faculty of Graduate and Postdoctoral Studies

Acute Injury of Hippocampal Dentate Gyrus and Hilus by Elevated External Potassium

By: Cristina Basile

This thesis is submitted as a partial fulfillment of the M.Sc. program in Cellular Molecular Medicine

September 22nd, 2005

University of Ottawa

Your file Votre référence
ISBN: 978-0-494-18396-0
Our file Notre référence
ISBN: 978-0-494-18396-0

Abstract

Potassium is the most abundant ion species in the mammalian central nervous system. Under normal physiological conditions, most K^+ in the brain tissue resides within the cytoplasm of neurons, glia, and axons. However, brain injuries such as trauma or ischemia may cause large amounts of K^+ to leak out. This sudden increase of K^+ in the interstitial space may have severe pathological consequences. Animal models suitable for studying K^+-mediated tissue injury are uncommon in the literature. Therefore, the main objectives of this thesis were: 1) to develop an animal model of K^+-induced tissue injury and 2) to examine the mechanism and cellular events that are potentially responsible for the observed tissue injury. We chose to study the dentate hilus (DH) of the hippocampus because previous studies have shown that K^+ homeostasis in this region is highly sensitive to traumatic brain injury.

Approximately 150 adult male rats were used throughout this study. Under anesthesia, a small volume of K^+ solution was injected into either the left or right hippocampal hilus. This was followed by an injection of the vehicle solution into the corresponding DH region of the contralateral hippocampus. The animals were then sacrificed at different time points post-K^+ or drug injections. Tissue sections were collected for immunofluorescent processing and quantification. The main findings are the following:

1) Microinfusion of low concentrations of K^+ into the DH produced, within minutes, a large tissue cavity along the subgranular zone (SGZ). The SGZ is mainly composed of the initial segments of mossy fibers from granular cells of the dentate gyrus, interneurons of the hilus and astrocytes.

2) The occurrence of the tissue split was accompanied by rapid injury and destruction of glial cells. There was no detectable death of granular neurons.
3) The K^+-induced tissue split can be reliably reproduced by the injection of the Na^+,K^+-pump inhibitor ouabain, which led to a rapid, endogenous increase of K^+ in the extracellular space (ECS). However, injections of equal volume of NaCl, $CaCl_2$ or distilled water did not induce tissue split in the DH.
4) In the presence of K^+ channel blockers, both ouabain and exogenously applied K^+ were no longer effective in producing the tissue split.

Based on the above results, it is concluded that the tissue integrity of hippocampal dentate hilus is extremely vulnerable to high external K^+. Glial cell death seems to play an important and early role in the occurrence of K^+-induced tissue damage. Since traumatic brain damage as well as temporal lobe epilepsy exhibits similar pathophysiological features to K^+-induced tissue injury, we propose that the latter can be used as a useful animal model for future mechanistic and therapeutic investigations.

Table of Contents

List of Figures

List of Abbreviations

4-AP	4-aminopyridine
α	alpha
ACSF	artificial cerebrospinal fluid
AMPA	α-amino-3-hydroxy-5-methyl-4-isoxazol-propionic acid
AQP	aquaporin
APP	amyloid precursor protein
atm	atmospheric
ATP	adenosine triphosphate
β	beta
Ca^{2+}	calcium ion
CA1-3	cornu ammonis 1-3
CNS	central nervous system
Cl^-	chloride ion
Cs^+	cesium ion
DG	dentate gyrus
DH	dentate hilus
dH_2O	distilled water
EAA	excitatory amino acid
EC	entorhinal cortex
ECS	extracellular space
E_K	equilibrium potential for potassium
EtBr	ethidium bromide

FPI	fluid percussion injury
GS	glutamine synthetase
GFAP	glial fibrillary acidic protein
GLT	glutamate transporter
H^+	hydrogen ion
ip	intra-peritoneal
IL	interleukin
K^+	potassium ion
KCl	potassium chloride
Kd	potassium dissociation constant
K_{IR}	inwardly rectifying potassium channels
GCL	granule cell layer
IFN	interferon
mRNA	messenger ribonucleic acid
msec	millisecond
MSO	methionine sulfoximine
Na^+	sodium ion
NaCl	sodium chloride
NMDA	N-methyl-D-aspartate
NOS	nitric oxide synthase
PB	phosphate buffer
PBFI	potassium-binding benzofuran isophthalate
PBS	phosphate buffered saline

ROS	reactive oxygen species
SE	standard error
SGZ	subgranular zone
TBI	traumatic brain injury
TCA	tricarboxylic acid
TEA	tetraethylammonium
TNF	tumor necrosis factor
VSOAC	volume-sensitive organic anion channel

Acknowledgments

I would firstly like to thank my supervisor, Dr. Bin Hu, for taking me on as his student. His invaluable knowledge and guidance provided an immense foundation on which to start my career in research.

I would also like to thank Dr. Leo Renaud for becoming my co-supervisor and providing me with a location to continue my project and studies and for allowing me to begin a new field of research in his laboratory.

Secondly, I would like to thank the members of the lab: Dr. Ayman Omar, Dr. David Mooney, Li Zhang and Caroline Cedrone for all their assistance and their friendship.

Lastly, I would like to thank my parents, sisters and husband for encouraging and supporting me throughout my graduate work and also for their continuous love and support.

Chapter 1

General Introduction

1. Traumatic Brain Injury and Temporal Lobe Epilepsy

Each year, an estimated 50,000 Canadians (Statistics Canada, 1996) and a million and a half Americans (Santhakumar et al., 2001; Esselman et al., 2004) suffer a traumatic brain injury (TBI) which is the leading cause of death and disability among citizens under the age of forty (Annegers and Coan, 2000). One of the major consequences of TBI is an increased incidence of temporal lobe epilepsy (TLE) and unprovoked seizures often years after the original TBI event (Anneger and Coan, 2000; Santhakumar et al., 2001). Cognitive disturbances and memory decline are also commonly seen among TBI patients (Santhakumar et al., 2001; Schwarcz and Witter, 2002). The mechanism of TBI remains poorly understood but new evidence suggests that it may be due to the specific injury of the dentate gyrus region within the hippocampus (Santhakumar et al., 2001; Schwarcz and Witter, 2002).

Post-mortem examinations of brains from TBI patients often reveal selective damage to the hippocampus, or more specifically, to the dentate hilus (DH) (Margerison and Corsellis, 1966; Toth et al., 1997). This region consists of mossy fiber projections from the dentate granular neurons to the CA3 region of the hippocampus as well as several types of GABAergic interneurons and astrocytes. The cells in the DH play a central role in the regulation of the input-output functions of the entire hippocampus (Buzsaki et al., 1983; Toth et al., 1997) and the post-traumatic injury of these neurons is thought to be an important factor in the development of trauma induced temporal lobe epilepsy (Doherty and Dingledine, 2001; Coulter et al., 1996; Toth et al., 1997).

1.1 Early Biochemical Responses to TBI in the Hippocampus

1.1.1 Large Increase in Extracellular K^+

Fluid percussion injury (FPI) is a widely adopted experimental model of TBI. In this model, the fluid percussion device delivers a brief (20msec), 2.0 to 2.2atm impact on the intact dura. The FPI-induced pressure waves lead to immediate tissue damage and behavioral deficits comparable to that induced by concussive trauma and penetrating head injuries (e.g. A bullet entering the brain can result in damage far away from the missile tract) (Ross and Soltesz, 2000; Lowenstein et al., 1992; Toth et al., 1997; Santhakumar et al., 2000).

The cellular mechanisms that trigger TBI-induced tissue damage remain a mystery. In order to deduce the events that trigger TBI-induced tissue injury, many laboratories have used microdialysis probes to measure changes in ion concentrations following TBI. One consistent finding is that when FPI is delivered to the head, it results in a massive increase of extracellular K^+ concentration within minutes (Katayama et al., 1990; Di et al., 1996; D'Ambrosio et al., 1998; Xiong and Stringer, 1999; Reinert et al., 2000). The K^+ concentration can surge from ten to thirty fold above the baseline level (approximately 3 mM) in a mere 2-3 minutes (D'Ambrosio et al., 1998; Xiong and Stringer, 1999). This initial rise is often followed by a later, more moderate increase that is concurrent with the occurrence of cortical spreading depression. This increase in extracellular K^+ has been shown to promote the generation of seizures by increasing neuronal excitability (D'Ambrosio et al., 1998; Xiong and Stringer, 1999).

In an early study by Katayama (1990), it was found that a mild FPI resulted in a small K^+ increase (1.40 to 2.15 fold above baseline levels) within the hippocampus whereas a more

pronounced insult resulted in a more severe, longer lasting increase (4.28 to 5.9 fold above baseline levels). This massive K^+ efflux is associated with a concomitant release of excitatory amino acids, namely glutamate, occurring immediately after the injury, which may further increase the concentration of extracellular K^+ by enhancing neuronal discharges.

In a study reported by D'Ambrosio and colleagues (1998), it was shown that FPI caused an immediate increase in the concentration of extracellular K^+. Later on, this group proposed that this enhanced accumulation of extracellular K^+ in post-FPI hippocampal slices could be caused by an exaggerated release of K^+ from hyperactive neurons, a decreased uptake of K^+ by astrocytes or a combination of both (D'Ambrosio et al., 1999). The post-FPI slices used in this study showed an elevated extracellular K^+ baseline concentration and exhibited altered neuronal activity. To demonstrate that the post-FPI mediated loss of K^+ conductance within astrocytes was similar to a drug mediated blockade, they used cesium (Cs^+), a pharmacological blockade which prevents K^+ uptake by astrocytes in uninjured slices. With this blockade they discovered an increased extracellular K^+ accumulation within the slice demonstrating that the loss of uptake of K^+ by astrocytes can greatly contribute to the massive increase of extracellular K^+ seen after TBI. Overall, it has been proposed that TBI causes a loss of K^+ conductance in hippocampal astrocytes, subsequently impairing K^+ homeostasis and neuronal function.

Another typical pathophysiological change accompanying TBI that may contribute to an increase in extracellular K^+ is the loss of certain types of K^+ channels within astrocytes. After injury, it has been found that there is a significant reduction in the expression of inwardly rectifying K^+ (K_{IR}) channels, a channel type that is abundantly expressed in astrocytes within the CNS (Kettenmann et at., 1993; D'Ambrosio et al., 1999). K_{IR} channels

are open at the resting membrane potential in astrocytes and are essential in mediating the diffusional uptake of K^+ (see below). Inhibition of these channels or a down-regulation in their expression can diminish the ability of the astrocytes to buffer extracellular K^+ (Bordey and Sontheimer, 1998; D'Ambrosio et al., 1999).

1.1.2 Axonal Disconnections

Axonal disconnection is an early pathological change following TBI. It is a result of direct neurofilament and cytoskeleton damage caused by acceleration and deceleration forces (Meythaler et al., 2001) which initiate secondary and Ca^{2+} dependant injurious events. Axonal injury and disconnections were originally thought to occur immediately after TBI due to tearing but it is now known that this tearing rarely occurs (Povlishock and Jenkins, 1995). Rather, axonal disconnection involves a traumatically induced disruption of the axonal membrane and eventually allows for an unregulated entry of Ca^{2+} which initiates a series of proteolytic processes by which the cysteine proteases, calpains and caspases can modify the axonal cytoskeleton causing irreversible damage (Maxwell et al., 1997; Singleton et al., 2002).

Singleton and colleagues (2002) recently examined FPI-induced axonal injury at short time points. At 30 minutes post-FPI, they observed axonal swelling in the thalamus, neocortex and hippocampus (as seen by APP immunoreactivity, an amyloid precursor protein specifically seen in damaged axons (Stone et al., 1998)). After two hours, it was found that only a few of the injured axons were still continuous with their downstream segments. At the 4-6 hour time points, all visualized reactive axonal swellings were disconnected, as there was no continuity seen between the APP positive cell bodies and their distal axonal segments.

The axotomized neuronal somata continued to exhibit normal morphology at the light microscope level with no obvious cell shrinkage, swelling or nuclear alteration even though the axonal damage was as close as 20-50μm to the soma (Singleton et al., 2002). When they looked closely at the hilar region, they were surprised to find out that this axotomy did not result in cell death of the dentate granular neurons although cell-cell disruption may have consequences on K^+ homeostasis (D'Ambrosio et al., 1999).

1.1.3 Selective Loss of Hilar Neurons

In various animal models, it has been reported that TBI does induce specific and selective damage to the GABAergic interneurons within the hilus and DG (Lowenstein et al., 1992; Toth et al., 1997; Santhakumar et al., 2000; Buckmaster et al., 2002). The same population of cells is also severely damaged in humans after brain injury and resembles "hippocampal sclerosis", a hallmark of temporal lobe epilepsy (Golarai et al., 2001). Hilar interneurons control the input-output function of the DG. In the post-TBI period, damage of hilar GABAergic interneurons was found to be accompanied by an enhanced excitability of the DG, providing a potential mechanism for TBI-related temporal lobe epilepsy (Toth et al., 1997; Santhakumar et al., 2001).

In an initial study by Toth and colleagues (1997), it was found that FPI led to a loss of hilar neurons by 58.7% ± 1.8% one week after the injury. To further investigate the acute and immediate damage to this region of the brain, they analyzed the hippocampal sections 50-60 seconds after an FPI insult. To detect injury to neuronal processes occurring quickly after an insult, they used the Gallyas stain, a silver stain used for neuropathological examination, and found that the hilar interneurons were stained intensely whereas the

surrounding granule cells remain unstained. The control animals, in which no FPI was performed, had all their neurons remain completely unstained. This may indicate that the injury caused by TBI preferentially impacts large cells that are not tightly packed in a cell layer as they are in the granule cell layer explaining the selective vulnerability of the hilar cells (Coulter et al., 1996; Toth et al., 1997; Lewén et al., 1999; Santhakumar et al., 2001).

The GABAergic hilar interneurons within the DH are injured within minutes following a fluid percussion injury to the cortex. This pressure wave caused immediate physical damage to both hilar cells and the pyramidal cells in the granule cell layer and this injury does not require the recruitment of any active physiological processes (Toth et al., 1997). Another hallmark found with FPI was an alteration in axons in as little as four to six hours after the injury was presented with dramatic cell changes seen after 24 hours (Singleton et al., 2002).

1.2 Cavity Formation Associated with TBI

Unlike traumatic injury in the spinal cord, TBI does not often lead to cavity formation. Fitch et al. (1999) found that after an injection of zymosan (to evoke an inflammatory reaction) into the brain, a large cavity occurred around the injection site. The intense inflammatory responses seen within their study is also a model for cavitation seen after TBI. The area of the cavity was completely devoid of both astrocytes and neurons but contained plenty of damaged axon ends along its borders. These cavities often progressed and got larger possibly as a result of active astrocyte migration and morphological changes of neurons due to the abandonment of their processes by the migrating astrocytes. The damage done to the axon by the process of cavitation was irreparable even with the eventual filling of

the wound with astrocytes and blood vessels (Singleton et al., 2002).

2. K^+ Homeostasis and Buffering

Mammalian cells maintain a large transmembrane gradient for K^+ (130 mM inside vs. 3 mM outside), which has very high membrane permeability. One of the most important features of neuron-glia interactions is related to the ability of glial cells in buffering extracellular K^+ (Amédée et al., 1997; Bordey et al., 2000; Walz, 2000). K^+ concentration fluctuates in the close vicinity of neurons following even a brief period of excitation (Hiruma et al., 1999) and if this increase is sustained and remains uncorrected, it may have variety of effects on neuronal excitability. It has been shown that an increase of extracellular K^+ to only 5 mM is enough to change the action potential threshold of hippocampal neurons, leading to hyperexcitability and impaired synaptic transmission (Balestrino et al., 1986; Kreisman and Smith, 1993).

One would expect that an immediate re-uptake of K^+ by neurons would be sufficient to prevent a build-up of excess extracellular K^+. However, this mechanism appears too slow to prevent K^+ build-up from affecting synaptic transmission and axonal ion channel kinetics (Walz, 2000). Instead, Hertz (1965) postulated that astrocytes must play a primary role in K^+ clearance from the extracellular space (ECS). There are three interrelated mechanisms for astrocyte-mediated K^+ buffering: the spatial diffusion mechanism, K^+ uptake via both the Na^+,K^+-ATPase pump and the Na-K-2Cl co-transporter, and passive uptake through KCl co-transporters (Walz, 1999).

2.1 Spatial Buffer Mechanism

The spatial buffer theory was formulated by R.K. Orkand in 1966. It rests on the assumption that astrocytes have a resting membrane potential that approximates the equilibrium potential for potassium (E_k); they have a high permeability for K^+ and are coupled to each other through gap junctions (Orkand et al., 1966; D'Ambrosio et al., 1998). These features would allow astrocytes to shuttle K^+ from a high concentration locus to a low concentration region therefore reducing K^+ in the ECS.

At the beginning of such a buffering mechanism, K^+ is first diffused into the astrocyte from the high concentration site via K^+ channels, especially the inwardly rectifying K^+ (K_{IR}) channels (see above). The K_{IR} channels are not only abundantly expressed in astrocytes in the adult hippocampus (Bordey et al., 1998) but have a high open probability at the resting potential and their conductance increases with an increase in extracellular K^+ concentration (Bordey et al., 2000). Furthermore, activation of K_{IR} channels promotes the influx of K^+ but impedes K^+ efflux (D'Ambrosio et al., 1998). As a result of increased K^+ entry, the local membrane potential of astrocyte will depolarize, thereby creating an electrochemical gradient that drives K^+ towards more negative regions of the astrocyte network distal from the site of K^+ entry (D'Ambrosio et al., 1998; Leis et al., 2005). Since astrocytes have very long processes and are connected through gap junctions, they can dump K^+ ions well away from the source of increase (Amédée et al., 1997). This method requires no energy from the astrocytes and is one of the major *in vivo* routes for K^+ buffering in the mammalian CNS (Walz, 2000).

2.2 Uptake of K^+ through the Na^+, K^+-ATPase and the Na-K-2Cl

2.2.1 The Na^+,K^+-ATPase pump

The Na^+,K^+-ATPase pump is an integral membrane protein expressed on both neurons and glia. Through the hydrolysis of adenosine triphosphate (ATP), the pump provides the energy for the asymmetrical pumping of two K^+ ions into the cell and three Na^+ ions out into the ECS. Such ion translocation is essential for the maintenance of Na^+ and K^+ transmembrane gradients in all cells of higher eukaryotes. A decrease in energy supply, such as during anoxia and ischemia, leads to the rapid cessation of pump activity and collapse of Na^+ and K^+ ion gradients (McGrail et al., 1991; Lingrel et al., 1994; Scheiner-Bobis, 2002).

The Na^+,K^+-ATPase pump is a complex structure containing both α and β subunits which function together as a dimer. There are three isoforms of the α subunit (α_1, α_2, and α_3) as well as three for the β subunit (β_1, β_2, and β_3). The α subunit is the catalytic unit of the enzyme. It contains the ATP binding domain, a phosphorylation site and amino acid sequences essential for binding cardiac glycosides and cations. The α_2 and α_3 isoforms are found mostly in neurons while the α_1 and to a lesser extent the α_2 isoforms are found on glial cells (McGrail et al., 1991). The α_2 and α_3 subunits are significantly more sensitive to the pump blocker ouabain than α_1 (O'Brien et al., 1994). The β subunit is involved in the maturation of the enzyme including its correct assembly into a stable configuration and aids in its targeting to the cell membrane (Lemas et al., 1994; Geering et al., 1996).

The functioning of the pump occurs as such: Firstly, three Na^+ ions located in the cytoplasm bind to the α subunit of the enzyme resulting in the enzyme being phosphorylated in a Na^+ dependent manner. The pump then undergoes a conformational change resulting in the exposure of the Na^+ binding sites to the ECS. The Na^+ ions are then released and two K^+

ions bind to the cation binding site of the pump. Once this occurs, there is a de-phosphorylation and conformational change back to the initial state of the enzyme. K^+ ions are released into the cytoplasm and the cycle is repeated. The net effect of the reaction cycle is the generation of a net negative potential of the inside of the cell relative to the outside of the cell (Glynne et al., 1990; Senatorov et al., 1997; Kandel et al., 2000; Senatorov et al., 2000). The neuronal Na^+,K^+-ATPase pump has a very high affinity for extracellular K^+ and is almost completely saturated at normal extracellular K^+ concentrations and is not usually affected by any extracellular increases. In contrast, in astrocytes the pump has a much lower affinity for extracellular K^+ and is therefore stimulated by increases in extracellular K^+ in the physiological and pathophysiological ranges (Walz, 2000). The astrocytic Na^+-K^+ pump is also stimulated by an increase in intracellular Na^+. Therefore, changes in internal Na^+ and external K^+ levels will both facilitate K^+ uptake in astrocytes. Since active ion pumping consumes energy, it is a less favorable mechanism for K^+ buffering (Amédée et al., 1997; Walz, 2000).

2.2.2 The Na-K-2Cl co-transporter

This co-transporter was originally found in astrocytes by Geck et al. (1980) when they showed that K^+ influx was blocked by loop diuretics (bumetanide and furosemide). Since its original identification, two separate isoforms from distinct genes have been cloned. The first isoform, NKCC1, has been shown to play an important role in astrocytic buffering of extracellular K^+ and cell volume regulation (Russell, 2000). The second isoform, NKCC2, which has restricted expression in certain segments of renal tubules, is involved in the reabsorption of salt in the kidney (Matthews, 2002).

The NKCC transporter proteins have twelve transmembrane spanning domains. The N-terminus is highly conserved through many species and contains a threonine phosphorylation site which is thought to be relevant to the overall functioning of the co-transporter. Both the amino and carboxy terminals contain multiple phosphorylation sites which regulate the action of this protein. Any ion translocation to the cytosolic side of the astrocytes requires that all three ions be simultaneously present on the extracellular side of the membrane (Russell, 2000; Matthews, 2002). This transport protein internalizes one Na^+, one K^+ and two Cl^- in an electroneutral coupled fashion.

When extracellular K^+ rises, it activates the Na-K-2Cl co-transporter which pulls all three ions into the cytoplasm of the astrocyte. This rectifies the action of the Na^+, K^+-ATPase which causes a drop in the concentration of intracellular Na^+. This transporter often runs outwards in epithelial cells but on astrocytes, it is only known to run inwards. The net effect is KCl accumulation, often accompanied by cell swelling due to an influx of water (Amédée et al., 1997; Walz, 2000; Su et al., 2001). To combat such a cell volume increase astrocytes can release excitatory amino acids (EAAs) through the activation of volume-sensitive organic anion channels (VSOACs) (Anderson and Swanson, 2000). The latter allows glutamate, together with Cl^- and other anions, to be discharged into the ECS. The molecular structure and function of VSOACs have not been fully characterized.

2.3 K^+ Uptake through the KCl co-transporter

Another K^+ buffering mechanism offered by astrocytes is through the KCl co-transporter (KCC). KCC belongs to the cation-chloride co-transporter superfamily. Four isoforms (KCC1-KCC4) have so far been identified with KCC2 being predominantly

expressed in the CNS. KCC operates in a bidirectional fashion and can therefore carry out net ion influx or efflux depending on the concentration gradient of the transported ions (Payne et al., 2003). The KCl co-transporter is a favorable mechanism for K^+ buffering since it does not require any energy from the astrocyte. This pump is also responsible for controlling cell volume (Walz and Wuttke, 1999; Walz, 2000).

3. Astrocytes and TBI

3.1 Astrogliosis

Within the first few hours of a brain injury, surviving astrocytes in the affected region begin to hypertrophy and proliferate, a process known as astrogliosis. Astrogliosis is common following a stroke or prolonged and frequent seizures (Bordey et al., 2000). Reactive astrocytes increase the expression of a structural protein, known as glial fibrillary acid protein (GFAP) (Eng et al., 2000). Their somata and processes become hypertrophic (Tanaka et al., 2002). D'Ambrosio et al., (1999) found that TBI induced an increase in GFAP immunoreactivity in post-traumatic glial cells, which appeared elongated with enlarged cell processes. This was also found in studies by Bordey et al., (2000) and Bordey and Sonetheimer (1998). At the area of injury, reactive astrocytes can interweave their processes to form a barrier and become an obstacle for regenerating axons (Chen and Swanson, 2003). Reactive gliosis is still a very complex phenomenon involving the interactions of several cell types with neurons which leads to neuronal survival or death and axonal regeneration or retraction (Ridet et al,. 1997).

4. Hypothesis

Although the disruption of K^+ homeostasis has been considered an important contributing factor to TBI and the subsequent development of temporal lobe epilepsy, very few studies have directly examined the potential cytotoxic effects of K^+ itself. We hypothesize here that a sudden surge of extracellular K^+ in the dentate region of the hippocampus may be directly involved in the induction of pathological changes observed during TBI. Since glial cells play an important role in acute tissue injury, we further postulate that high extracellular K^+ concentration may be particularly detrimental to the survival and function of glial cells.

5. Objectives

The goal of the research described herein was to test the hypothesis that a moderate to high level increase in extracellular K^+ can serve as a trigger or inducer for pathological changes resembling that induced by TBI. Our primary objectives are:

- to develop and evaluate an animal model of K^+-induced tissue injury and,
- to examine the mechanism and cellular events that are potentially responsible for the observed tissue injury.

We chose to study the DH because previous studies have shown that K^+ homeostasis in this region is highly sensitive to traumatic brain injury.

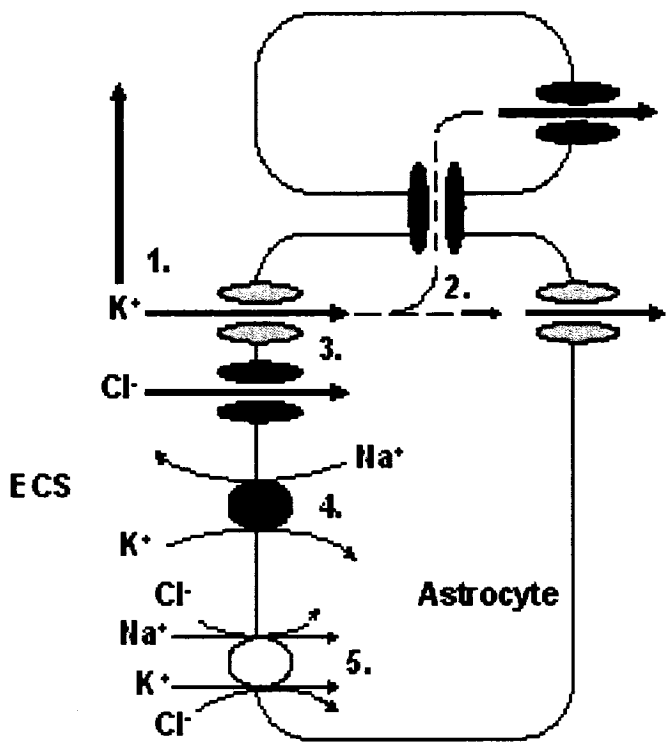

Figure 1.

Schematic diagram of the principal routes for buffering changes in extracellular K^+. 1. Extracellular diffusion. 2. Spatial buffering involving the passage of K^+ through gap junctions to a neighboring astrocyte. 3. Net uptake in along with Cl^- through the KCl channel. 4. Na^+,K^+-ATPase. 5. Na-K-2Cl co-transport. ECS = extracellular space.

Chapter 2

Animal model of K^+-induced tissue damage in rat hippocampus

METHODS

Animal Preparation

The anesthesia, surgical and experimental protocol adopted in this study was approved by the Ottawa Hospital Animal Care Council, which ensures conformity with the guidelines of the National Institutes of Health and the Canadian Council on Animal Care. Detailed experimental procedures were published before (Omar et al., 2000; Omar et al., 2001; Omar, 2002). Briefly, male Long-Evans rats (150-175g) were anesthetized with Somnotol (0.12 ml/kg body weight, ip) and mounted on a stereotactic frame. Two symmetrical burr holes were drilled on each side of the skull at stereotactic coordinates corresponding to the dentate gyrus (Bregma: -3.8, Lateral: 2.4) (Paxinos and Watson, 1998). A Hamilton microsyringe was lowered to the upper blade region of the dentate gyrus (ventral to the dura: -3.3), which was filled with either of the following solutions: The experimental side was injected with KCl with concentrations ranging from 5 to 50mM, 0.5mM ouabain (Sigma-Aldrich), 5 to 100mM NaCl, 5 and 10mM Ca^{2+}, 0.5μM charybdotoxin (Alomone), 100mM TEA + 50mM 4-AP (Sigma-Aldrich; RBI), 4mM kyneurenic acid (Sigma-Aldrich), and distilled water (dH_2O). The control side was injected with saline (0.9% NaCl) or artificial cerebrospinal fluid (ACSF) (124mM NaCl, 3.2mM KCl, 26.2mM $NaHCO_3$, 1.3mM $MgCl_2 \cdot 6H_2O$, 1.0mM NaH_2PO_4, 10mM glutamate, 2.4mM $CaCl_2 \cdot 2H_2O$). All solutions were slowly infused at a rate of 0.5μl/minute for 4 minutes (2μl total). The microsyringe was left in place for 20 minutes after the injection to prevent any back diffusion of the injected material. The wound was closed with 4-0 prolene sutures and the rats were allowed to regain consciousness. Temgesic (0.02mg/kg) was given for post-operative analgesia.

Figure 2.1. Hippocampal locations of K^+ Injection

Coronal section of adult rat hippocampus. Two symmetrical burr holes are drilled on each side of the skull at stereotaxic coordinates corresponding to the dentate gyrus (Bregma: -3.8, Lateral: 2.4). A Hamilton microsyringe is first lowered to the upper blade region of the dentate gyrus (ventral to the dura: -3.3) and then into the corresponding region on the contralateral side of the brain as control. ML = molecular layer, H = hilus, GCL = granule cell layer, CA1-3 = cornu ammonis 1-3. Scale bar represents 500μm.

Tissue processing

At various time points following the injections (5 minutes to 4 hours), the rats were anesthetized using the same procedure as previously mentioned and transcardially perfused using 60ml of cold saline (0.9% NaCl) to flush the vasculature followed by 250ml of 4% paraformaldehyde (w/v) in 0.1M phosphate-buffer (PB) (0.2M monosodium phosphate, 0.2M disodium phosphate, pH 7.4) with 4% sucrose (w/v). The rats were decapitated, whole brains removed and post-fixed overnight at 4°C in the same fixative with 20% sucrose (w/v). Brains were cryosectioned at 40μm spacing and approximately 25 sections were collected per animal and were immediately floated with gentle agitation in the same fixative solution with 10% sucrose (w/v) for 30 minutes. The sections were subsequently washed (3 x 5 minutes) in 0.02M PB + saline (0.9% NaCl) (PBS) and placed in a 5% skim milk (in 0.02M PBS) blocking solution containing 0.3% Triton X-100 (BDH) for one hour at room temperature. They were then placed in their respective primary antibodies (anti-GFAP (Promega) at 1:250; anti-neurofilament-200 (Sigma-Aldrich) at 1:250) all in 0.02M PBS + 0.3% Triton X-100 and incubated with rotation overnight at 4°C. The following day, the sections were washed with 0.02M PBS (3 x 5 minutes) and incubated with the appropriate secondary antibody (ALEXA 488 goat anti-rabbit IgG (Molecular Probes) at 1:1000; ALEXA 488 goat anti-mouse IgG (Molecular Probes) at 1:1000) in 0.02M PBS for two hours at room temperature and in the dark. Sections were then subsequently washed with 0.02M PBS and mounted on slides. After drying, a drop of Prolong Anti-fade (Molecular Probes) was applied to each section and they were sealed with a coverslip before any imaging was performed.

Detection of *In Vivo* K^+ Signal

Potassium-binding benzofuran isophthalate (PBFI) (Molecular Probes, USA) is a membrane impermeable dye and was used here as a new method for the detection of extracellular K^+ *in vivo*. PBFI was co-injected with various concentrations of K^+ or with 0.5mM ouabain in the same manner as described previously (Omar et al., 2000; Omar et al., 2001; Omar, 2002). At different time points (5 minutes to 4 hours), the animal was sacrificed. Since PBFI is highly hydrolic and can be easily washed out from tissue section during perfusion, we avoided this problem by quickly removing and freezing the brain unperfused using an isopentane solution (Fisher Scientific, Canada) and storing the tissue at –80°C. The tissue was then cryosectioned as mentioned above and placed directly on a slide.

To obtain quantitative measurements of PBFI signals using intact tissue sections, a dose-response relationship between PBFI and extracellular K^+ concentration must be first determined. To this end, we used normal Long-Evans rats (150-175g; Charles River, Canada). Once fully anesthetized they were decapitated and the brain was immediately frozen using isopentane (Fisher Scientific, Canada) and cryosectioned at 10μm spacing. The sections were then placed on a gelatin coated slide and allowed to dry. Afterwards, a drop of PBFI (0.5mM) containing different concentrations of K^+ (2, 3, 5, 10, 20, 30, 40, 50, 75 and 100mM) was placed directly on the brain slice and allowed to incubate for 10-15 minutes after which any excess liquid was removed. Although PBFI is described as K^+ selective, its potassium dissociation constant (K_d) is strongly influenced by Na^+ concentration. To mimic physiological conditions *in vivo*, 100mM Na^+ was added to the solution containing K^+ and PBFI.

Analysis of Fluorescence Intensity

Tissue sections were examined at 5x, 10x and 20x magnification using an OLYMPUS fluorescence microscope and analyzed by Northern Eclipse (version 6.0) software. For PBFI, fluorescence analysis was performed by exciting the indicator at 340nm and emission measured at 500nm (manufactory specifications). The fluorescent images were captured and the total fluorescent yield was analyzed using Northern Eclipse (version 6.0) software which line-scans an area of fluorescence and plots the results as a grey scale value (pixel value) from 0-255 (where 0 is the darkest and 255 is the brightest). The mean (±SE) fluorescent values were plotted against the corresponding K^+ concentration used. This generates a standard calibration curve enabling one to determine the concentration of K^+ based on fluorescent intensity.

RESULTS

Part 1. K^+ Induces Tissue Split in DH

Potassium injections were performed in 45 rats where 2μl of K^+ and a vehicle control solution were injected bilaterally into the opposite side of dentate hilus areas of the hippocampus. In all of the animals injected with K^+, a large cyst-like tissue split on the side of potassium infusion was formed (Figure 2.2). This K^+-induced tissue split took place in less than 30 minutes and always occurred within the subgranular zone (SGZ) beneath the granular cell layer (GCL). Figure 2.3 summarizes the K^+ concentrations and post-injection time points that produced a tissue split in different animal groups. We found that in some rats even a 5mM K^+ injection caused a tissue split. Furthermore, no differences were found in terms of left versus right side of the hippocampus or between the rostral and caudal planes

of the hippocampus.

Part 2. K^+ Selectivity

In this set of experiments we examined whether the tissue split is selective to changes in external K^+ concentration. Besides using saline as the control, we also injected ACSF (n=3; 2μl), distilled water (n=3; 2μl), 100 mM NaCl (n=3; 2μl) and 5mM $CaCl_2$ (n=3; 2μl) into the same DH area. As shown in Figure 2.2, all of these monovalent and divalent ions failed to produce a tissue split. In the second set of experiments, we examined whether K^+ channel blockers could prevent the occurrence of a tissue split. We found that two types of K^+ channel blockers that act on Ca^{2+}-dependent (charybdotoxin; 0.5μM; n=15) or voltage dependent K^+ channels (TEA + 4-AP (tetraethylammonium + 4-aminopyridine) 15mM; n=9) were both effective in blocking the tissue split formation when they were co-injected with a high concentration of K^+ or ouabain (see below) (Figure 2.4). In contrast, the glutamate receptor antagonist, kyneurenic acid (4mM; n=3) was ineffective in blocking the tissue split (data not shown). These observations indicate that the tissue-split is very selective to increases in external K^+ concentration.

Part 3. Tissue split can be induced by ouabain and endogenously released K^+

Ouabain is a potent Na^+,K^+-ATPase blocker and its application leads to rapid loss of cytoplasmic K^+ as well as an increase in extracellular K^+ concentration (Erecinska and Silver, 1994; Lees and Leong, 1994; Balestrino et al., 1999; Li et al., 2001). The purpose of this series of experiments was to determine whether K^+ released endogenously from the cells could also cause a tissue split. As shown in Figure 2.5, ouabain injection invariably induced

a large tissue split between the GCL and the hilar region, similar to that induced by the K^+ solution. The split produced by ouabain appeared much larger especially when the rats were allowed to survive for a few hours. At the 4 hour time point, the tissue split extended over the entire upper blade of the dentate gyrus (Figure 2.5c). Also, following the ouabain injection, there was a drastic decrease in the number of GFAP positive cells within the hilar region (see below). Given the rats were under deep anesthesia, ouabain treatment did not give rise to apparent seizure activities. This was also the case for the K^+ injected rats. Furthermore, ouabain-induced tissue damage was restricted to the one side of the brain since injections of saline (Figure 2.5a) into the control side in the same animal left the entire hippocampus intact.

Part 4. Detection of extracellular K^+ using PBFI

A critical element of our overall hypothesis is the assumption that K^+, either applied exogenously or released internally from the tissue, must be present at the time of tissue damage. The high membrane permeability of K^+ and its susceptibility to various mechanisms of uptake (see Introduction) could in theory restrict the temporal and spatial capacities of K^+ rise in the extracellular space, therefore limiting its toxicity. There is currently no practical method that can adequately address these technical limitations, especially for estimating the spatial distribution of K^+ signals *in vivo*. In this part of my thesis study, I have explored whether PBFI can be used as a new method *in vivo* for monitoring K^+ distribution. PBFI is a membrane impermanent extracellular K^+ dye with high K^+ selectivity in the presence of physiological concentrations of other monovalent cations (Minta and Tsien, 1989). I first performed experiments to determine whether a

standard curve of PBFI fluorescence intensity could be constructed *in situ* in an intact brain section and used to estimate the concentration and spatial distribution of extracellular K^+. The procedures for this experiment are described in the Methods section. As shown in Figure 2.6, the standard curve constructed using this method indeed has a slope region of fluorescence increase when the external K^+ concentration was increased from 2mM to 100 mM. In the next set of experiments, PBFI and 5mM K^+ were co-injected into the DH (Figure 2.7), which induced a typical tissue split along the upper blade of the dentate gyrus. Strong PBFI fluorescent signals were observed in the area surrounding the tissue damage (Figure 2.7a). The averaged intensity of PBFI signals (231.16 ± 9.97 pixels^2) associated with the tissue split are however significantly higher than the value for 5mM estimated from the standard curve (209.57 ± 2.38 pixels^2) in normal tissue sections. We interpret this observation as the result of additional K^+ efflux from broken axons and/or damaged glia around the tissue split (see below). At higher magnification (Figure 2.7b), we observed strong fluorescent "filaments" interspersed within the granule cell layer. Although the nature of these filaments is unknown, we suspect astrocytes may play an important role in their formation (see below). Injections of PBFI alone produced no florescent signals in these experiments (Figure 2.7), indicating that the dye was not up-taken by non-injured cells and reacting with intracellular K^+. Co-injection of PBFI with 0.5mM ouabain produced similar results (Figure 2.7 c,d), indicating that PFBI is also capable of detecting K^+ released endogenously from injured neuronal elements. The lack of widespread of K^+ signals following local ouabain application suggests that potential secondary neuronal responses (such as seizures or spreading depression) did not give rise to large increase in external K^+ concentration outside the DH.

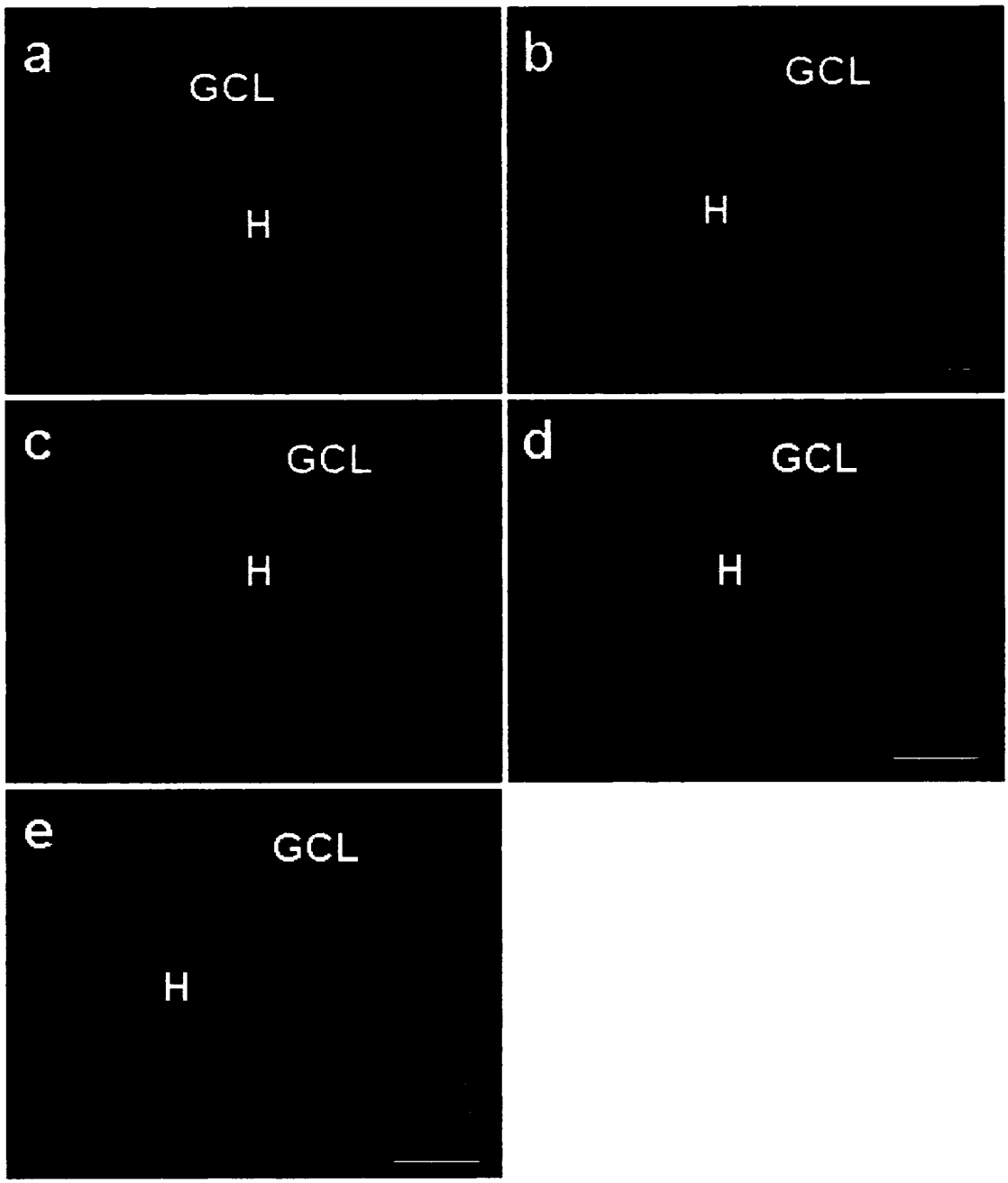

Figure 2.2 K^+ Selectively Induces Tissue Split in DH.

Coronal sections of hippocampal brain slices obtained 2 hours post-injection with various solutions. (a-c) GFAP staining; (d and e) bright field images. (a) Large tissue split in DH region after an injection of 5mM K^+. (b) Injection of ACSF. (c) Injection of saline, (d) Injection of 100mM NaCl. (e) Injection of 5mM Ca^{2+}. Note that only K^+ caused the large area of tissue damage. The tissue cavity in (c) is part of the lateral ventricle between the hippocampus and thalamus. Scale bar: 250μm. GCL: granule cell layer and H: hilus.

Summary of K^+ Injection Experiments

	50mM K^+	25mM K^+	15mM K^+	5mM K^+
½ hour	4			
1 hour	4			
2 hours	4			
1 hour		4		
2 hours		4		
1 hour			4	
2 hours			4	
5 min				6
15 min				6
1 hour				4
2 hours				4

Figure 2.3 Summary of Different Animal Groups Used in This Study

The numbers in the graph indicate the number of rats used for each concentration group. All the potassium injected rats included here have shown a typical tissue split in the DH along the SGZ.

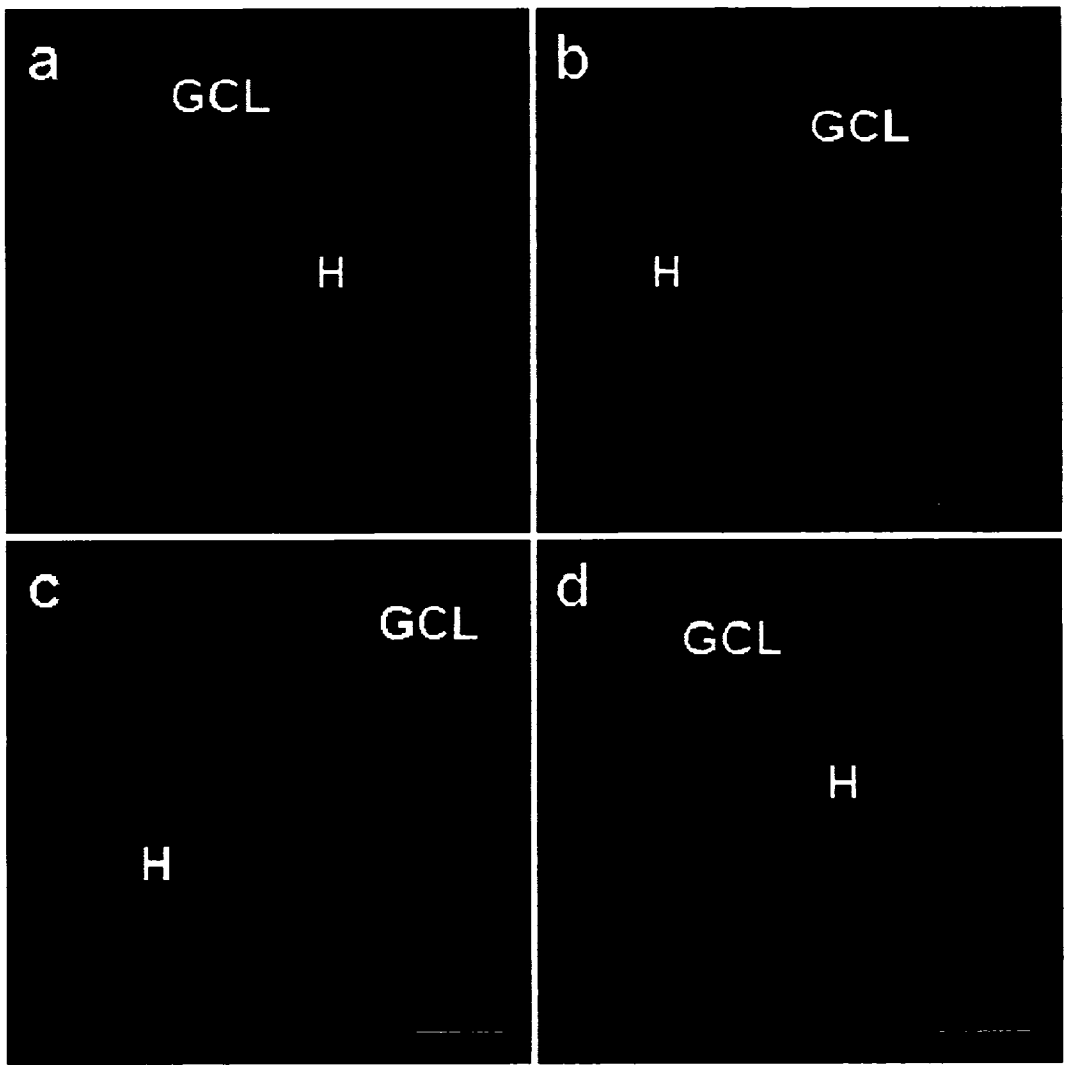

Figure 2.4 K^+ channel blockers prevent tissue split.

Coronal sections of hippocampal brain slices. (a) Five hours after an injection of 0.5mM ouabain into DH and the appearance of a large tissue split as well as loss of GFAP positive cells. (b) In the same animal 0.5mM ouabain was co-injected with 0.5μM charybdotoxin on the contralateral side. Note the absence of the tissue split as well as the preservation of GFAP positive cells. (c) Tissue split induced after a 15mM K^+ injection (2 hour survival time). (d) Co-injection of 15mM K^+ with TEA + 4-AP prevents tissue damage and loss of GFAP positive cell. Scale bar: 250μm.

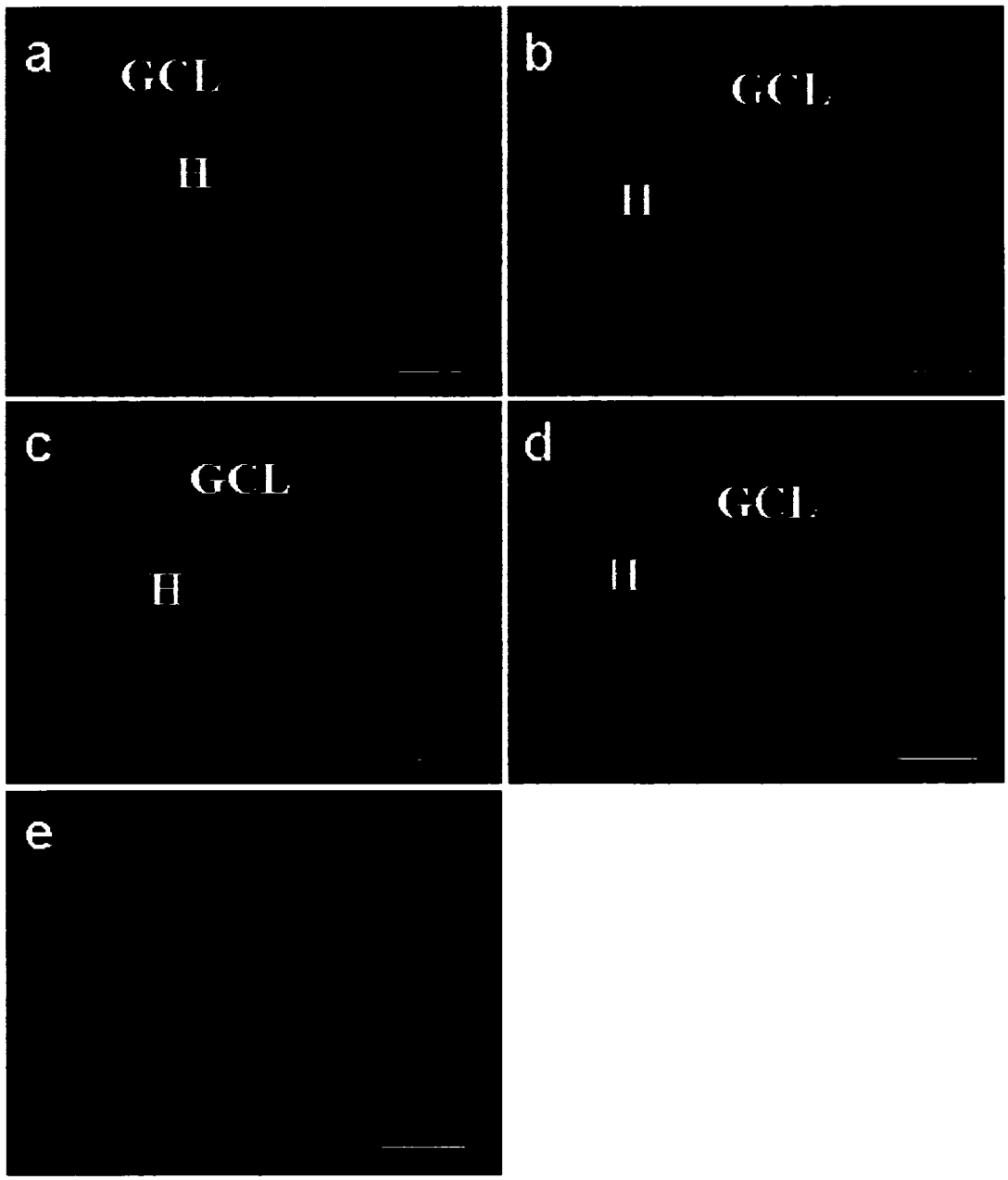

Figure 2.5 Tissue Split Induced By Ouabain

All the images are from coronal hippocampal sections immunostained for GFAP. (a) Representative tissue section with saline injection. The DH region has maintained its normal morphological appearance. The cavity in the right hand corner is the part of the lateral ventricle between the hippocampus and thalamus. (a-e) 0.5mM ouabain was injected and rats were left to survive for: (b) 1 hour, (c) 2 hours, and (d) 4 hours. (e) Primary antibody omission control. Scale bar: 250μm. GCL: granule cell layer and H: hilus.

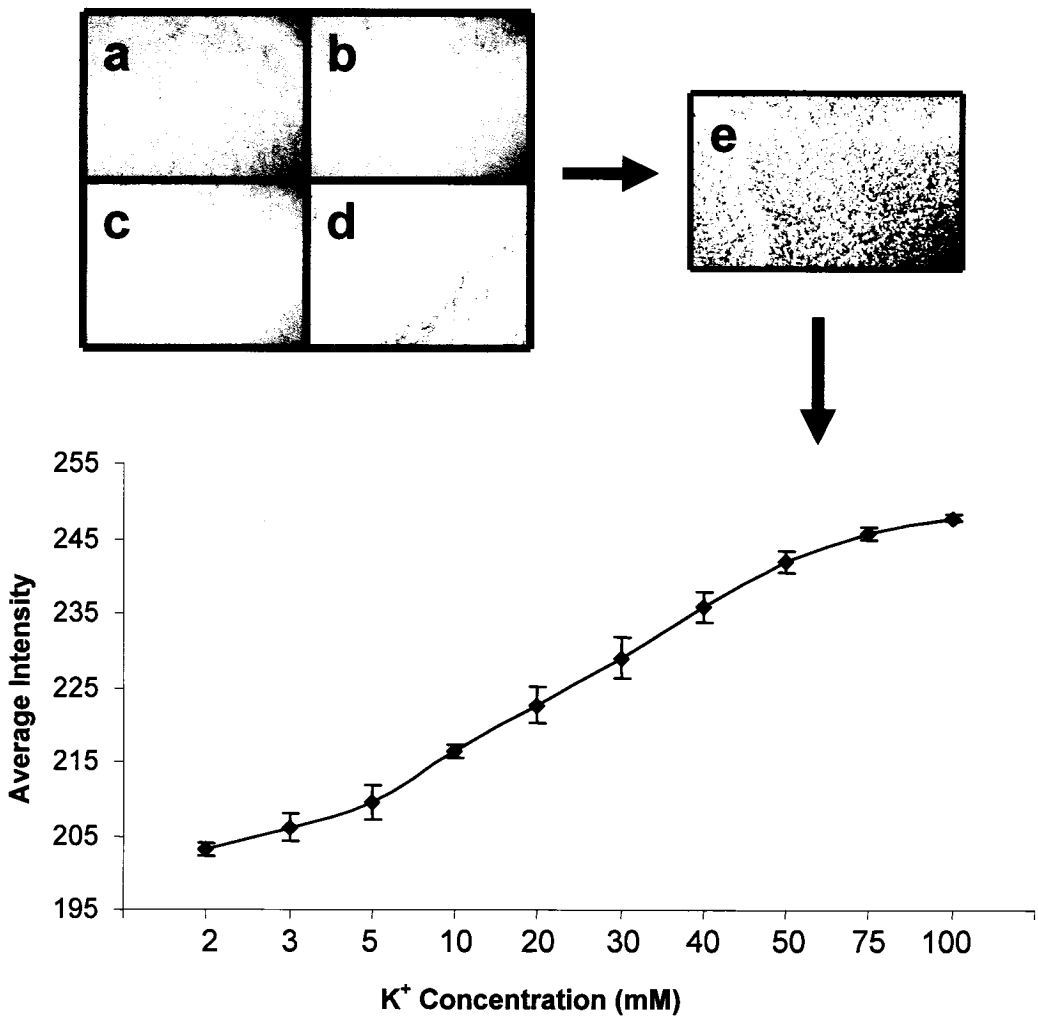

Figure 2.6 Standard Fluorescence Response Curve of PBFI with Different K^+ Concentrations in Tissue Slices

Fluorescence images of PBFI were first captured in the presence of 5 to 100 mM K^+ (a-d) for each section. The brightness indicates high PBFI signals (comparing a with d). Each fluorescence image is then converted into a grayscale image (e). Based on the grayscale images, the average intensities (in $pixels^2$) of PBFI fluorescence were calculated. The mean (±SE) intensity was plotted against K^+ concentrations, generating a standard curve. The integration (exposure) time for all the pictures was the same.

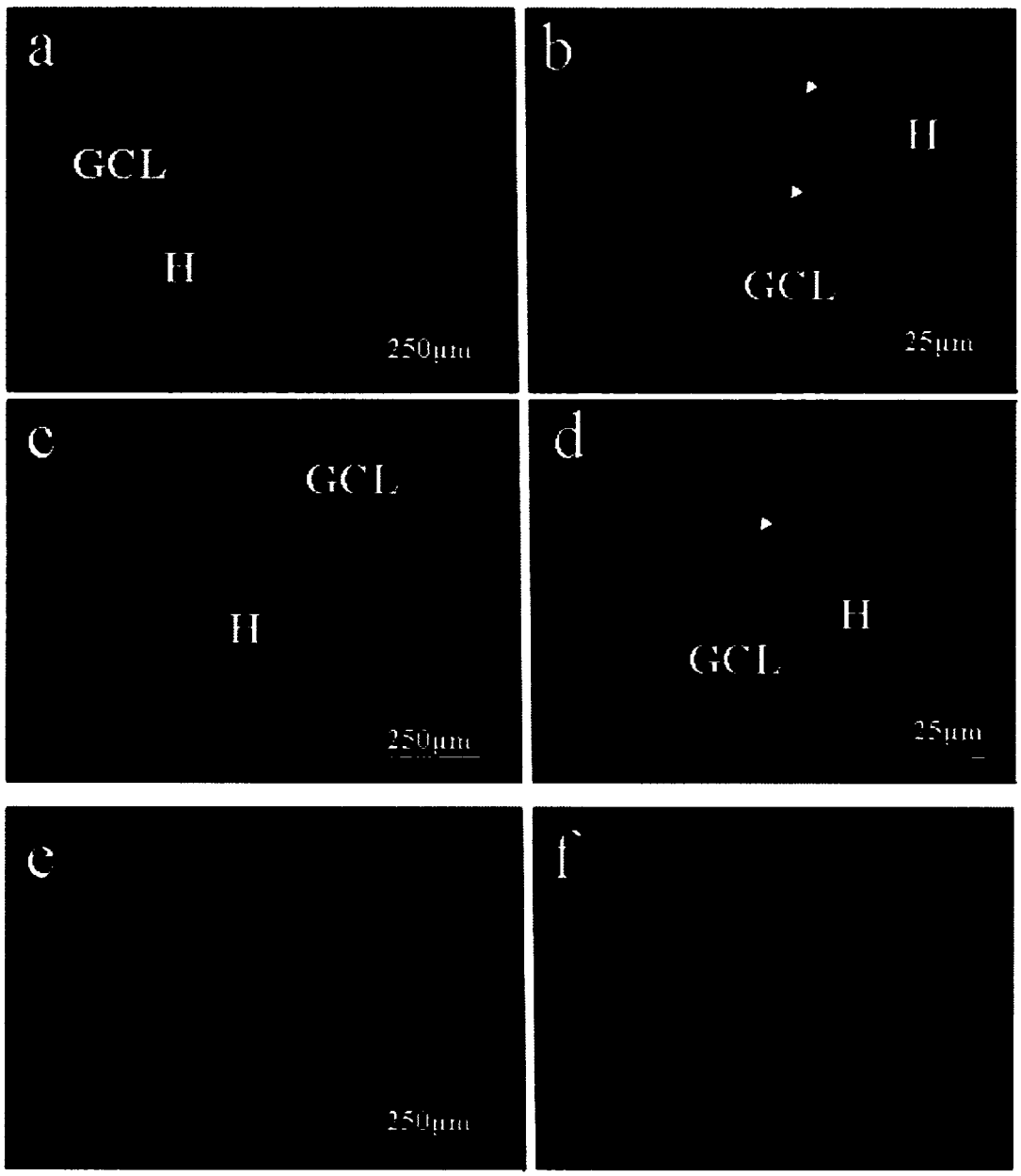

Figure 2.7 Increase In Extracellular K^+ During Tissue Split

Coronal sections of hippocampal brain slices. (a) PBFI (0.5mM) was co-injected with 5mM K^+. High level of fluorescence signals appear around tissue split. (b) High magnification image of (a) showing PBFI "filaments" (arrows) formed in the GCL. (c) Co-injection of 0.5mM ouabain and PBFI. (d) High magnification image of (c). (e) Injection of PBFI without ouabain or K^+ reveals only background level of PBFI fluorescence at physiological level of extracellular K^+. (f) Injection of K^+ without PBFI.

Chapter 3

Mechanism of K^+-induced tissue split: the role of astrocytes and potassium channels involved.

METHODS

Animal Preparation

The animal preparation, anesthesia and injection protocols are identical to that described in Chapter 2. The only modification was that 40μM ethidium bromide (EtBr) (Molecular Probes) was used in addition to other chemicals to detect cell death.

Fluorescence and Confocal Imaging Analysis

For analyzing thin astrocyte processes and PBFI fluorescence filaments, the brain tissue was cryosectioned at 10μm and placed directly on slides. Once dried, the sections were examined at 5x, 10x and 20x magnification. The images were captured by an OLYMPUS 1x70 fluorescence microscope and analyzed by Northern Eclipse (version 6.0) software. For confocal analysis, images were taken at a 60x magnification by a Bio-Rad 1024 confocal laser scanning microscope (Olympus) using a 60x oil-immersion objective (Olympus Optical, Tokyo, Japan). Digitized images were analyzed using BioRad-1024 and Image J (version 1.28) software. The diameter of the astrocyte filaments were calculated using this software. Similar treatment groups were averaged and compared against other groups. The area of the soma of the astrocyte was also calculated and compared with other treatment groups. All data are presented as mean ± SE.

RESULTS

Glial cells play a pivotal role in K^+ homeostasis and maintenance of tissue structural integrity. We have noticed that the appearance of a tissue split and rise in extracellular K^+ were often associated with a drastic reduction in GFAP signals (Figure 2.2 and 2.4). In this

set of experiments, we performed a quantitative analysis of this phenomenon. The results are reported as the following.

Part 1. Time dependent loss of glial cells during K^+ or ouabain-induced tissue injury

As illustrated in Figures 2.1(b,c), 2.4(a) and 3.1(a), in normal hippocampal tissue GFAP staining reveals a well organized glia network in the DH and SGZ regions. On average, between 100 and 120 GFAP positive cells were observed within the hilar region in every 40μm slice. A large number of GFAP positive fibers transverse through the SGZ and radiate into the granular cell and molecular layers (Figures 3.1(a) and 3.2(a)). Injections of K^+ (especially at higher concentration) or ouabain caused a significant reduction in GFAP staining and loss of GFAP positive cells (Figures 3.1 and 3.2). We counted total number of GFAP cells in each section under different treatment conditions. It was found that glial cell loss is particularly severe at 4 hours post-injection (>80% cell loss) although cell damage can take place as early as 30 minutes (Figure 3.3). The high vulnerability of astrocytes to ouabain or elevated K^+ treatment is in sharp contrast to the neurons in GCL where no apparent cell loss is encountered at the 4 hour time point (also see Discussion) (Omar et al., 2000; Omar, 2002; Cedrone et al., 2005).

Part 2. Structural changes of single glial cells

Since astrocytes play a key role in maintaining external potassium (Amedée et al., 1997; Bordey et al., 2000; Walz, 2000; Leis et al., 2005) we sought to further characterize structural damage in individual astrocytes at a single cell level using confocal image analysis. As shown in Figure 3.4, all the glial cells we examined exhibited significant swellings in

both somata (n=24) and processes after ouabain injection (Figure 3.4). By 2 hours the somatic area of individual astrocytes had increased by 4 fold (Figure 3.4(c)). Such severe and persistent swelling may impose high mechanical stress upon the cell membrane and cytoskeleton and subsequently predispose astrocytes for structural breakdown (see below). Consistent with previous studies (Walz and Wuttke, 1999; Bordey et al., 2000), we have also observed that GFAP levels are increased in ouabain injured astrocytes (Figure 3.4 (b)). However, this overexpression of GFAP was transient and mainly observed at the 2 hour time point. It seemed to recede back to control level prior to massive loss of glial cells at the 4 hour time point.

Part 3. Potential role of glial cells in tissue split

In a normal tissue section, a large number of glial cells are present in the hilar region with their processes transversing the SGZ and granular cells zone into the molecular layer (Figure 3.5 (a)). In this part of thesis I examined how glial cell injury may contribute to the formation of a tissue split. High magnifications of confocal images were acquired at different stages of the tissue split in GFAP sections. The most consistent change I found was a "break up" of glial cells associated with the tissue split. As shown in Figure 3.5, after a 15mM K^+ injection, many isolated GFAP positive processes appeared in the GCL. These elements were no longer attached to the cell bodies that remained in the hilar region on the opposite side of the tissue split. This feature of cell injury is consistent with structural damage as a result of mechanical stretch rather than apoptotic or necrotic cell death, both of which do not typically show soma-process separations. Two lines of evidence further suggest that mechanical stress may contribute to the formation of a tissue split. Firstly, as

shown in Figure 3.6, the diameters of GFAP positive processes were increased by over 30% (from 1.2 to 1.6μm) after ouabain injection, likely due to cell swelling. Interestingly, the average diameters of PBFI filaments were found to be very similar to that of glial processes. We interpret this correlation as caused by an influx and accumulation of PBFI dye into the broken processes, although the astrocytic nature of the PBFI filaments remains to be confirmed in future experiments. Secondly, if tissue swelling and mechanical tearing contributes to the tissue split, axons of neurons in the hilus must exhibit certain forms of disconnections from the somata. Indeed, staining using a neurofilament antibody revealed frequent disconnections of the axons and neuronal somata around the tissue split (Figure 3.7).

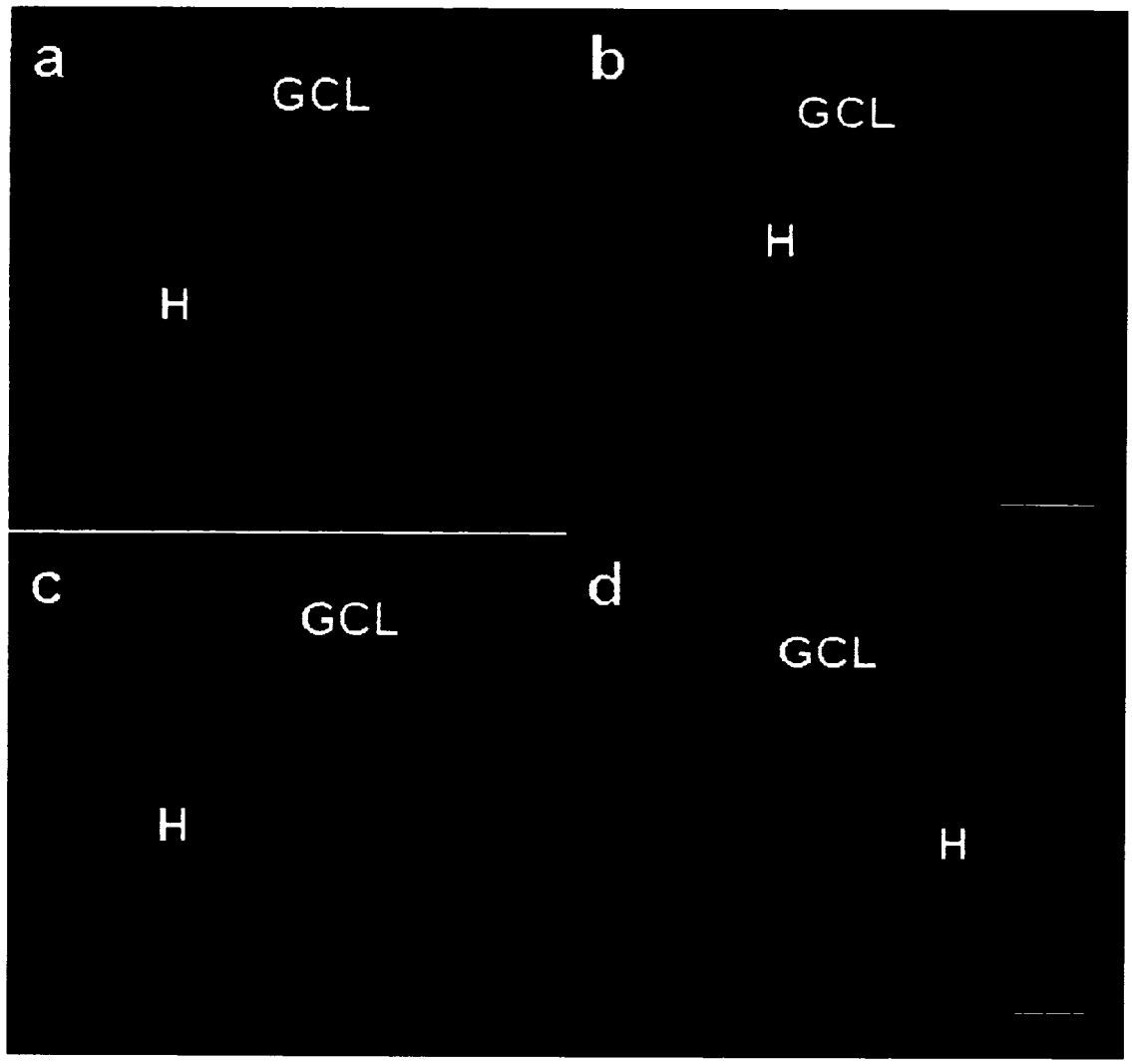

Figure 3.1 Loss of Astrocytes Following K^+ Injection

Coronal sections of hippocampal brain slices. GFAP stained sections showing K^+-induced cell injury. (a) Saline control. Note number of glial cells and the radiations of GFAP-positive processes. (b) Ethidium bromide co-injection with 5mM K^+ (post injection time=30 minutes). Note the rapid cell death (red fluorescence) occurring around the tissue split. (c) 50mM K^+ injection with 2 hour incubation period induces large tissue split and loss of GFAP positive cells. (d) 5mM K^+ injection with 5 minute incubation period. Note the significant preservation of GFAP-positive cells despite the tissue split. Scale bar: 250μm.

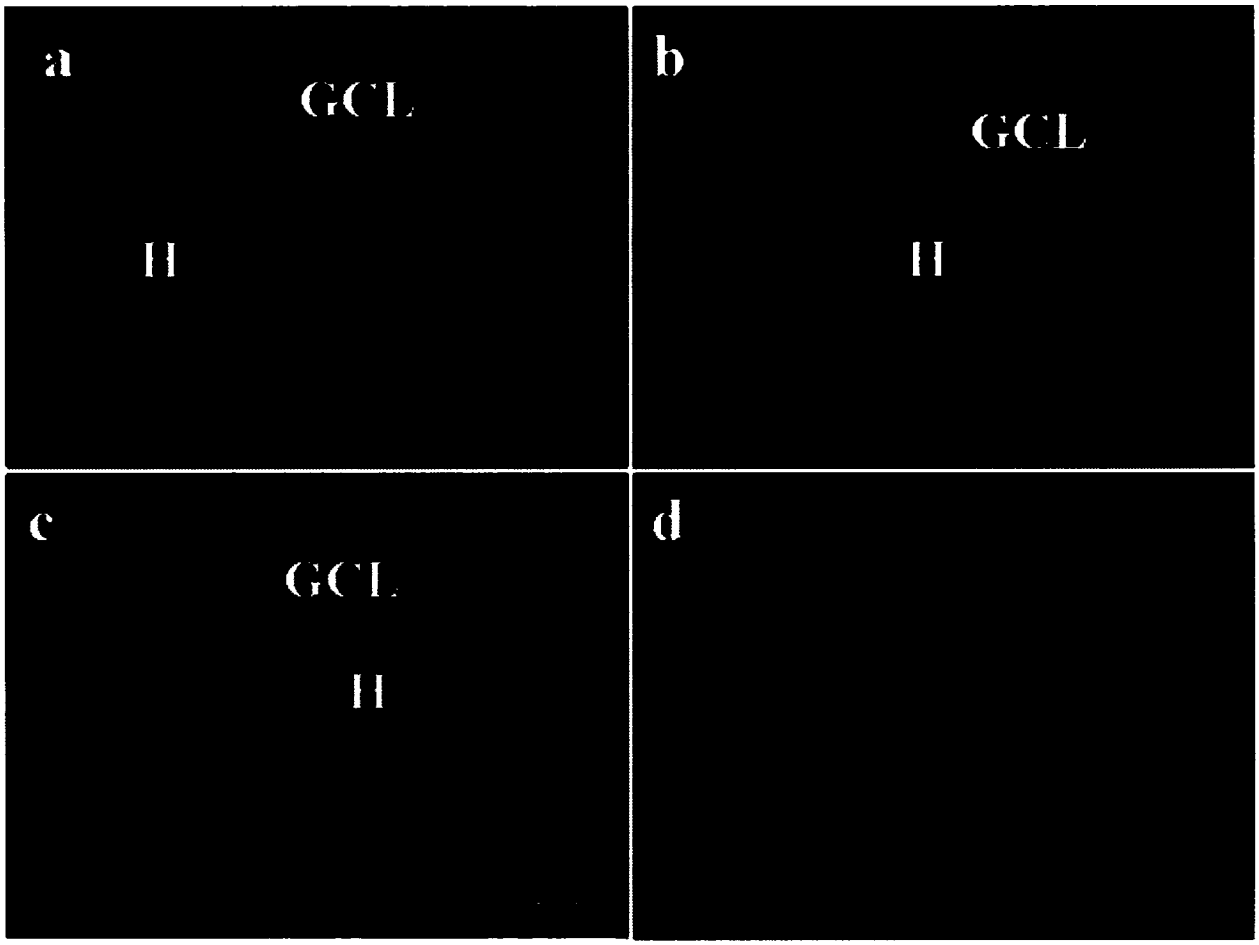

Figure 3.2 Loss of Astrocytes Following Ouabain Injection

Coronal sections of hippocampal brain slices stained with GFAP showing ouabain-induced cell injury. (a) Saline injection control (with lateral ventricle shown on the lower right hand corner). (b) 1 hour after an injection of 0.5 mM ouabain. Note the decrease in the number of GFAP positive cells and processes in the DH region. (c) 4 hours after the 0.5 mM ouabain injection. (d) Primary antibody omission control. Scale bar: 250μm.

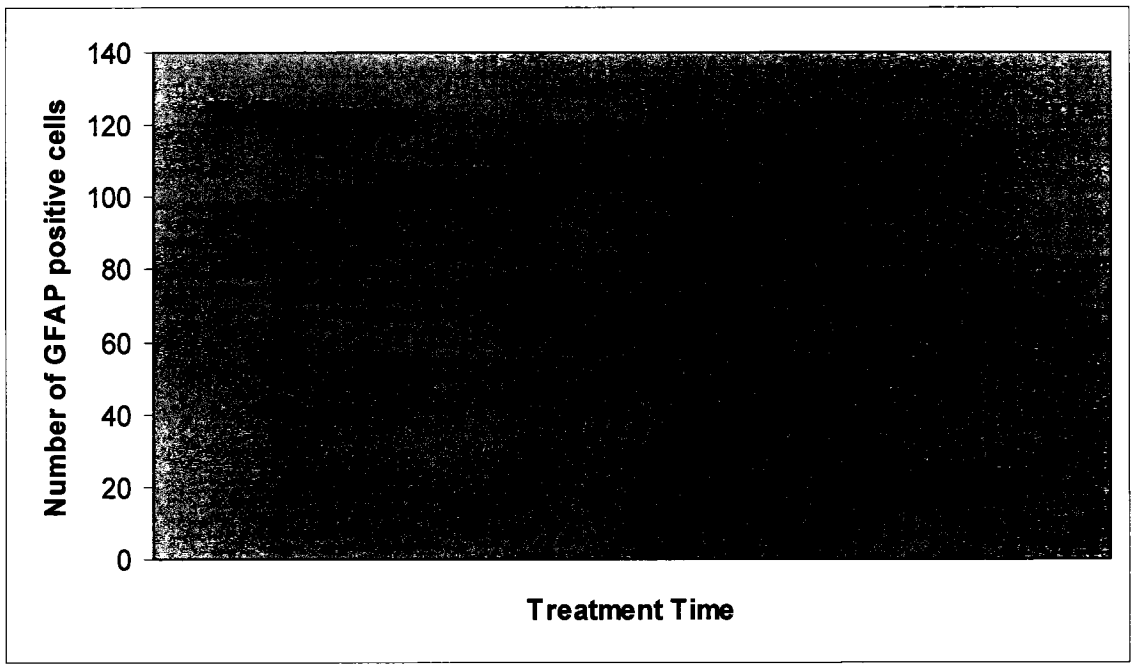

Figure 3.3 Time-Dependent Loss of Astroctyes after Ouabain Treatment

Data is derived from 25 rats. GFAP-positive cells were counted from multiple slices and averaged for each time point post-ouabain injection (0.5mM). They are shown as Mean ± SE.

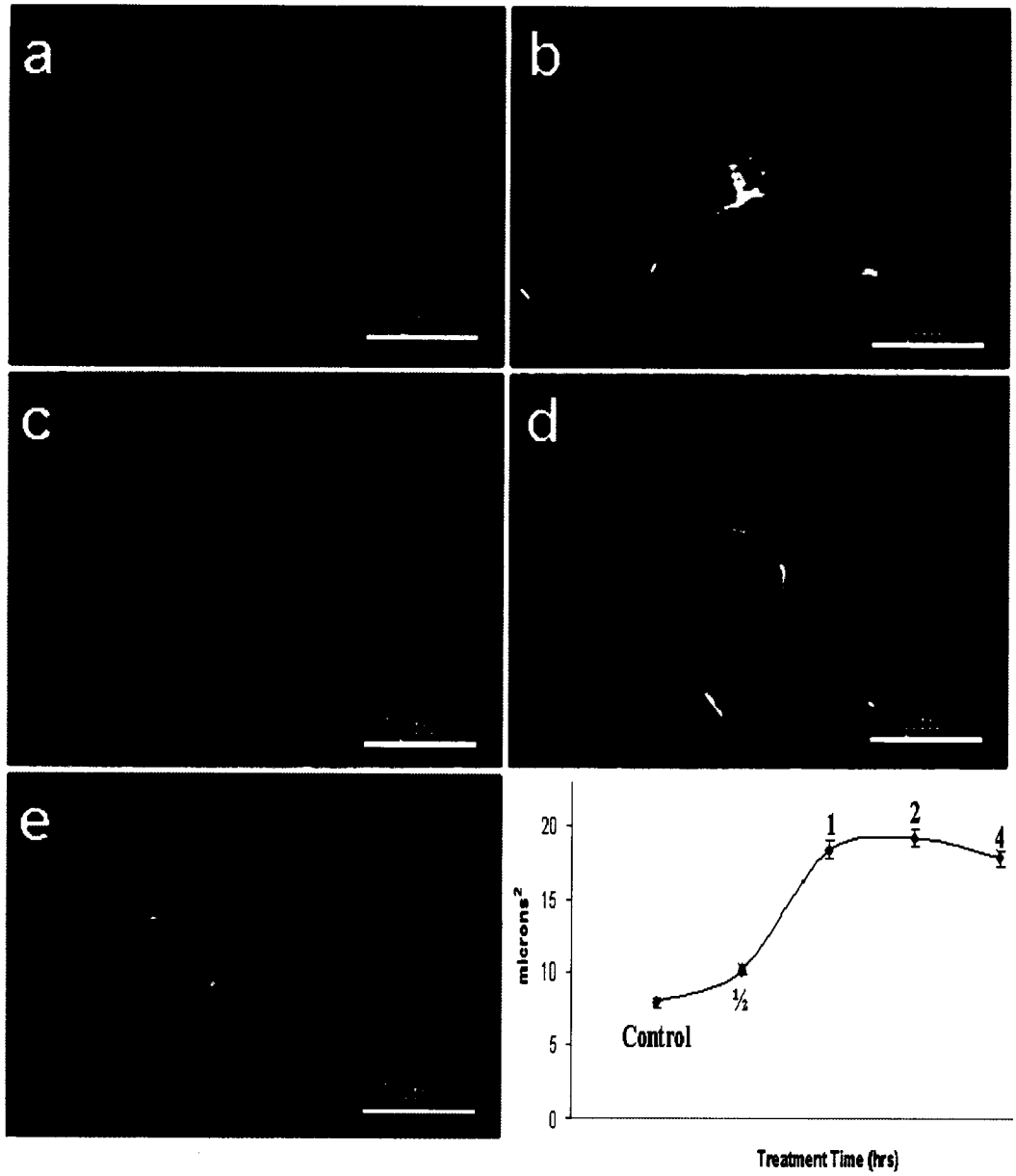

Figure 3.4 Swelling of astrocytes after endogenous K^+ release

(a) Normal GFAP positive astrocytes with 3-4μm in diameter. (b) ½ hour after 0.5mM ouabain injection. (c) 1 hour, (d) 2 hours, (e) 4 hours after the injection. (f) Summarized data on cell swelling, measured as the area of the somata (Mean ± SE) at different post-treatment time. The cell bodies more than double in size, a common feature of astrogliosis. Scale bar=5μm.

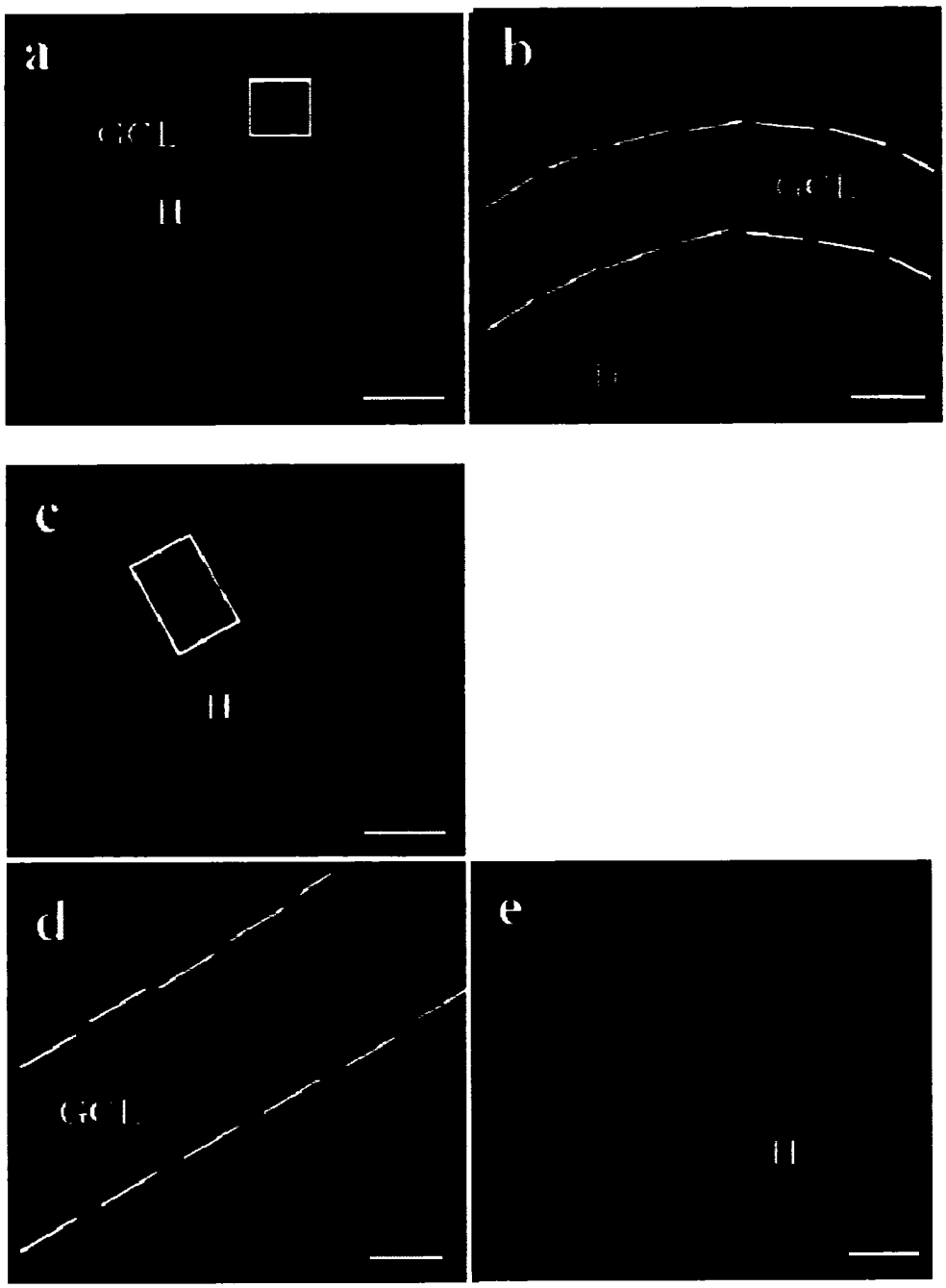

Figure 3.5 GFAP Processes Are Broken Across the Area of Tissue Split.

(a) Control tissue section with saline injection. Notice the abundance of (b) High magnification (60x) view of GFAP positive cells in the hilar region and their processes transversing the GCL. (c) 10x magnification view of the hippocampal tissue split 15 minute after an injection of 15mM K^+. Notice the higher level of GFAP signals following K^+ injection. (d) Detailed view of the boxed area in (c) showing that the GFAP positive processes in the GCL that are no longer attached to the cell body (denoted by the red arrow in (h)), which remains in the hilar region after the tissue split occurred.

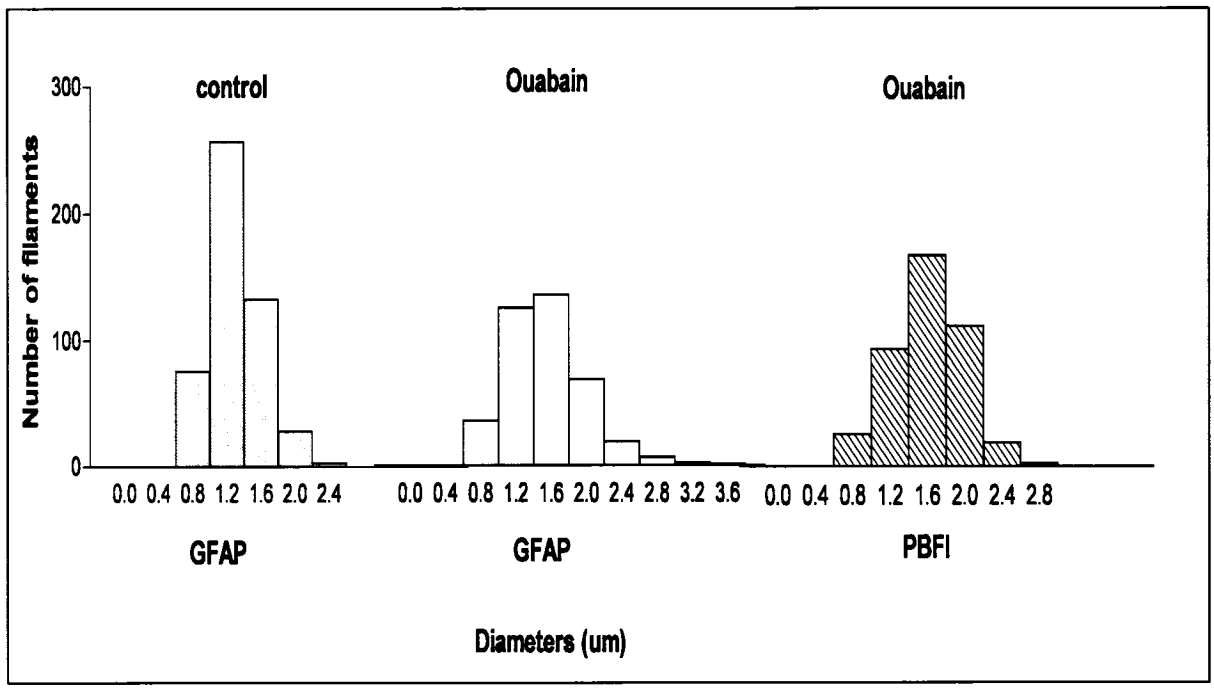

Figure 3.6 Quantitative Analysis of GFAP Processes and PBFI Filaments.

The diameters of GFAP positive processes and PBFI filaments were measured and compared in histograms. The diameter of GFAP filaments under control conditions centers around 1.2 μm. After ouabain injection, the diameters of GFAP processes and PBFI filaments are both 30% thicker than the control with the center distributions around 1.6 μm.

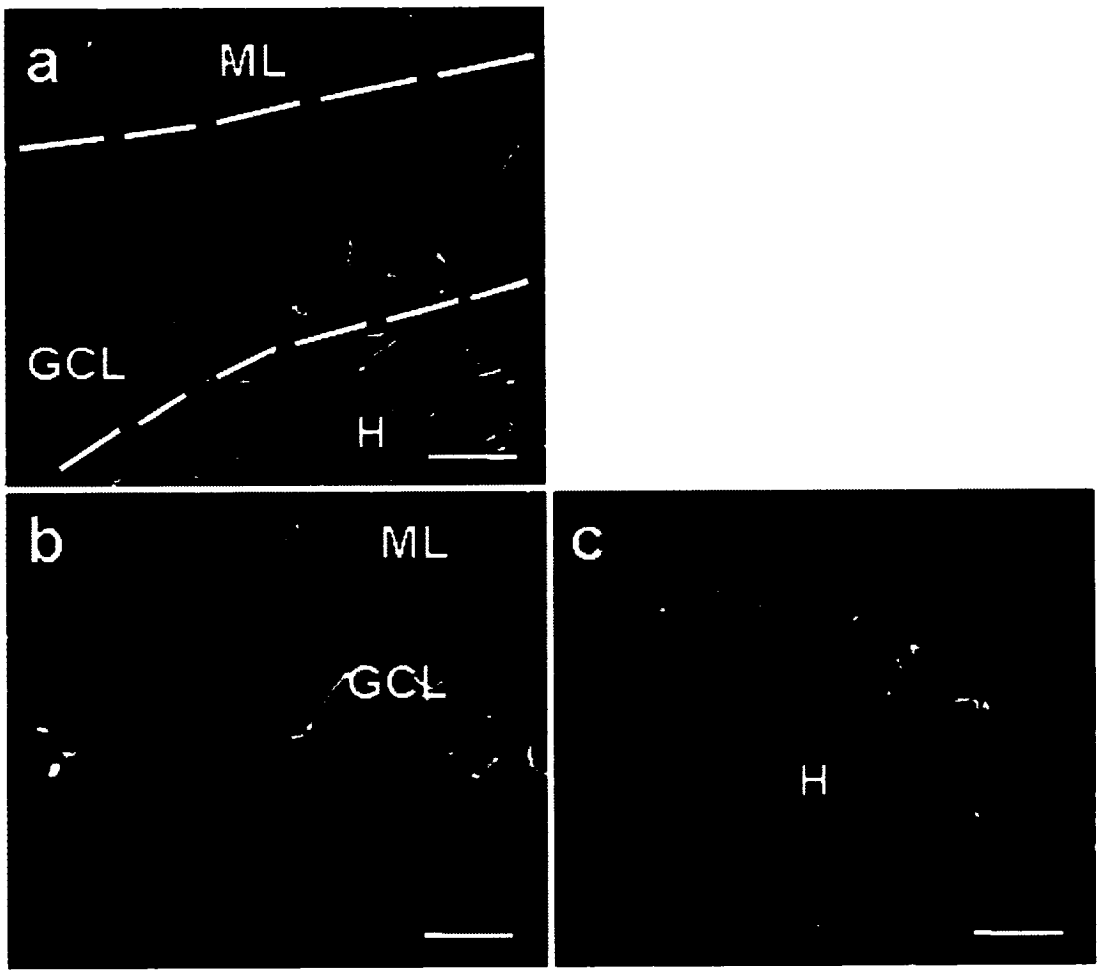

Figure 3.7 Neurofilament Processes Are Broken Across Tissue Split.

Coronal sections of hippocampal brain slices exhibiting neurofilament positive elements immunostained with NF-200 in the hilus. (a) Control brain slice. The cell body containing neurofilaments are seen in the hilus whereas the axons extend from the hilus into the GCL and molecular layer. (b) 30 min after a15mM K^+ injection results in a tissue split. The neurofilament processes are now found in the GCL but the cell bodies remain in the hilus (c). GCL: granule cell layer; ML: molecular layer and H: hilus. Scale bar represents 5μm.

Chapter 4

General Discussion

1.1 Thesis Objectives

The main objective of this thesis research was to establish an animal model for the investigation of direct cytotoxic effects caused by elevated extracellular potassium. We were interested in this model due to the following observations previously reported in the literature. Firstly, a rise of extracellular K^+ concentration is one of the earliest tissue responses associated with TBI, anoxia/ischemia and persistent epileptic discharges (D'Ambrosio et al., 1998; Xiong and Stringer, 1999; Leis et al., 2005). Large increases of extracellular K^+, ranging from ten to thirty fold above baseline levels, occur within minutes after these brain insults (Kawamata et al., 1995; Xiong and Stringer, 1999; Reinert et al., 2000). In animal models of TBI, disruption of K^+ homeostasis can persist for a long period of time after the initial brief insult (Toth et al., 1997). Secondly, K^+ can have both direct and indirect cytotoxic effects. For example, high K^+ is an important inducing factor of cell swelling, especially astrocyte swelling (see below) and a moderate rise in external K^+ has been shown to cause disruption of axonal transport (see below). Finally, an *in vivo* animal model is needed at this time to evaluate K^+ tissue toxicity. To this end, we designed the present thesis research. We report here several original observations on the possible cellular events involved in K^+-induced tissue injury. Below, I shall discuss various potential mechanisms of K^+ tissue toxicity and its clinical relevance. The discussion is divided into four parts: 1) Methodological considerations. 2) Possible mechanisms of K^+-induced cell injury. 3) Mechanism of the tissue split. 4) Relevance to TBI and epilepsy.

1.2 Methodological Considerations

1.2.1 Animal model and general methods

The hippocampus, which includes the entorhinal cortex (EC), the hippocampus proper, the dentate gyrus (DG) and the subiculum, plays a central role in memory formation and producing both short and long-term spatial memory (Small, 2002). The hippocampus appears to act as a memory buffer which consolidates long-term memory and the processes of new memory formation (Scoville and Mulner, 1957). In addition, the hippocampus plays a very important role in the association of complex multimodal sensory information and laying down new memory traces (Holscher, 2003). The hippocampus was chosen for this thesis work as many post-mortem examinations of brains from TBI patients revealed selective damage to this region, specifically, the dentate hilus. The post-traumatic loss of GABAergic interneurons in this area is thought to be an important factor in the development of trauma related epilepsy (Toth et al., 1997; Santhakumar et al., 2001; Schwarcz and Witter, 2002).

This work was performed in an *in vivo* setting and based on local applications of K^+ solutions. Hence, the natural progression of both cell and tissue damaging processes could be examined. Many of the caveats of conventional lesion techniques (e.g. artery occlusion) were avoided since focal infusion of K^+ solution has little influence on system functions including blood supply and the level of tissue oxygenation.

Glial fibrillary acidic protein (GFAP) was used throughout this study as an immunohistochemical marker for astrocyte identification (Ludwin et al., 1976; Eng et al., 2000). GFAP expression is required for astrocytes to perform functions such as modulating astrocyte motility and shape by providing structural stability to astrocytic processes and maintaining the integrity of the blood brain barrier (Eng et al., 2000; Chen and Swanson,

2003). This antigen allowed us to obtain a detailed visualization of glial cell location, somatic swelling and processes breakdown at single cell level using imaging techniques, particularly those associated with a tissue split. However, GFAP labeling does not permit us to investigate the roles of other non-neuronal cell populations, such as neural progenitor cells, microglia and macrophages, in the formation of a tissue split. There are also other markers for reactive astrocytes besides GFAP. The antibody J1-31 recognizes a protein which is associated with glial intermediate filaments. It specifically stains the reactive astrocytes adjacent to the area damaged by trauma (Malhotra and Shnitka, 1994; Ridet et al., 1997). An antibody has also been raised against the M22 antigen which is overexpressed in a population of highly reactive astrocytes located in areas containing extensive damage (Eddleston et al., 1996; Ridet et al., 1997). The antibody against 6.17 detects fibrous astrocytes of the white matter in the intact rat and all astrocytes after injury (Ridet et al., 1997). The use of these additional antibodies in future studies may provide new information about the fate of glia cell in K^+-induced tissue injury.

1.2.2 Measurement of Extracellular K^+ Levels

Under physiological conditions, the level of extracellular K^+ is around 3 mM. There are many circumstances under which K^+ ions can be released from the cytoplasm of neurons and into the extracellular space. For example, in the case of a single action potential, the resting level normally increases by approximately 1mM (Adelman and Fitzhugh, 1975; Walz, 2000). A train of artificial stimulation of neuronal pathways can increase external K^+ by about 5mM above the normal resting level. During seizures, the level can rise to approximately 12mM and during injury (hypoxia/ischemia and TBI) the concentrations can

reach up to the level of 25mM (Walz, 2000). The absolute extracellular K^+ concentration is also influenced by the volume of extracellular space.

One commonly used method in measuring extracellular K^+ concentration is through a potassium-sensitive double-barreled microelectrode. However, the microelectrode method does not allow for the estimation of the spatial extent of potassium released over a large tissue area, especially *in vivo*. Furthermore, a "dead space" is often created around the tip of the microelectrode that is several times larger than the extracellular space. As a result, the amount of limited K^+ release, such as during an action potential, can be severely underestimated. It has been suggested that one would get a more reliable estimate with the use of indirect methods (Walz, 2000).

The potassium-sensitive dye PBFI provides an alternative method for measuring extracellular K^+, particularly for *in vivo* experiments. The cell impermeant fluorescent probe consists of a fluorophore that is linked to the nitrogens of a crown ether with a cavity size selective for the K^+ ion although its affinity is affected by the presence of other monovalent cations in the intact tissue (Minta and Tsien, 1989).

When a solution of PBFI was combined with various concentrations of K^+ (100, 75, 50, 25, 10, 5, 3 and 2mM) and a fixed physiological concentration of Na^+, the mean intensity of PBFI fluorescence exhibited a slope region that roughly matched the external K^+ level we expected under experimental conditions (Figure 2.6). In terms of spatial and temporal resolutions, we found that PBFI can be used reliably to estimate the spatial spread of K^+ signals *in vivo*, even for detecting rapid potassium release.

1.3 Possible mechanisms of K^+-induced cell injury

1.3.1 K^+ toxicity

Under physiological conditions, extracellular K^+ concentration remains relatively constant. A transient surge in external K^+ does not in general impose immediate harm to the surrounding tissue. The maintenance of a low external K^+ level depends critically upon the activity of astrocytes, which utilize three parallel mechanisms to prevent large sustained K^+ accumulation in ECS: the Na^+, K^+-ATPase, the Na-K-2Cl co-transporter, and the passive diffusion of potassium through K^+ channels (Walz, 2000; Muller and Somjen, 2000).

In this study, in order to investigate the direct tissue toxicity of K^+, we used two methods to artificially elevate the external K^+ concentration. Both of these methods, K^+ injection and ouabain application, yielded similar results: i.e. rapid glia swelling and death, tissue split and disconnections of axonal and glial processes. In order to confirm that these methods indeed led to an elevated external K^+ for an extended period in the vicinity of the tissue split, we used PBFI to visualize K^+ signals across the DH area. When PBFI was co-injected with ouabain or 5mM KCl solution it was observed that a significantly higher level of extracellular K^+ could be detected along the upper blade or SGZ of the dentate gyrus where the tissue split usually took place (Figure 2.7). These observations indicate that high extracellular K^+ is clearly involved in the observed pathological changes. Two additional lines of observations provide further support to this assertion. First, we replaced KCl solution with ACSF, distilled water, NaCl or $CaCl_2$ and injected them in the same manner. None of these solutions were able to produce a tissue split as seen with K^+ (Figure 2.2). Second, the co-application of K^+ channel blockers completely prevented the tissue split formation induced by high K^+ and ouabain (Figure 2.4). On the other hand, the glutamate

receptor antagonist kyneurenic acid was ineffective in blocking the tissue split.

1.3.1.1 "Direct" mechanism of K^+ toxicity

We shall first consider two possible detrimental effects of high K^+: cell swelling and disruption of axonal transport.

K^+-induced astrocyte swelling is a common form of tissue injury in experimental models of TBI, epilepsy and ischemia/anoxia. It is generally believed that a relatively high concentration of K^+ (>50 mM) is required to induce significant tissue swelling. However, a recent *in vivo* study suggests that this may not be the case. Mori and co-workers (2002) have shown that after an occlusion of the carotid artery, a small and gradual increase in external K^+ (5-10 mM) can be induced *in vivo* within approximately 60 seconds. This rapid increase in K^+ is associated with a fast and significant reduction in cerebral ECS (Mori et al., 2002) suggesting that tissue swelling can occur very quickly and in parallel with only modest changes in external K^+ concentration. Astrocyte swelling triggered by high potassium also occurs rapidly in intact retina preparations. Interestingly, in this case, the processes of a swollen astrocyte often show shrinkage and elongation indicating that the morphological changes in astrocytes are complex and dynamic (Uckermann et al., 2004).

The mechanism of K^+-induced swelling in astrocytes is thought to be mediated by Na-K-2Cl co-transporters. When extracellular K^+ rises, the Na-K-2Cl co-transporter is activated pulling all three ions into the cytoplasm of the cell. The net effect is KCl accumulation and subsequent cell swelling due to the osmotically driven influx of water. Impaired extrusions of ions by a failure of the Na^+,K^+-ATPase pump or a higher production of cytosolic solutes by the breakdown of macromolecules may also contribute to the swelling

process (Chen and Swanson, 2003; Zhao et al., 2003). Interestingly, under the situation of high extracellular K^+, Na^+,K^+-ATPase activity does not lead to any significant changes in intracellular Na^+ concentration which is due to a transmembrane Na^+ cycle (Walz, 2000). Under conditions of high extracellular K^+, these ions are pumped into the astrocyte by the Na^+,K^+-ATPase. A simultaneous drop in intracellular Na^+ concentration is prevented by the stimulation of the Na-K-2Cl co-transporter allowing the Na^+ concentration to be replenished inside the cell. This cycle, which maintains a stable concentration of intracellular Na^+, provides the counter ion for the Na^+,K^+-ATPase ensuring that its activity remains continuous. The net effect of this entire process is only an accumulation of KCl and subsequent swelling due to an osmolyte increase (Walz, 2000; Walz, 1987). However, further studies are needed to determine the role of Na-K-2Cl co-transporters in the glia swelling observed in our experiments and whether this swelling and the occurrence of a tissue split can be blocked by a transporter blocker.

Water channels or aquaporins are the primary route for water entry into the astrocyte in response to osmotic stress (Venero et al., 2001). Aquaporins are membrane proteins that mediate the rapid transmembrane transport of water. Ten aquaporins have been cloned with only 1 and 4 located in the CNS. Aquaporin-4 is the predominant subunit expressed in astrocyte end-foot processes and plays a major role in brain water balance and K^+ buffering (Nagelhus et al., 1998). Mice lacking this protein show less astrocyte swelling under focal ischemic conditions (Manley et al, 2000). In the hippocampus of patients with temporal lobe epilepsy, a significant increase of AQP-4 was reported (Lee et al., 2004). This increase was correlated with an increase in GFAP expression and may contribute to the epileptogenic properties of the tissue (Lee et al., 2004).

Besides tissue swelling, Hiruma et al., (1999) have recently described another mechanism of "direct" K^+ toxicity. Using time-elapse and video-enhanced microscopy, these authors examined how the transportation of protein particles along dorsal root ganglion axons can be affected by extracellular K^+ concentration. It was found that increasing external K^+ from the control concentration by 5 mM inhibited both anterograde and retrograde axonal transport within a few minutes in a concentration-dependent manner (Hiruma et al., 1999). This blockade is persistent and requires the presence of external Cl^-. Therefore, it likely involves Na-K-2Cl transporters. Since axonal transport is vital in the maintenance of structure and function of the cytoskeleton, this finding may have important implications for understanding TBI-induced axonal damage.

1.3.1.2 "Indirect" mechanism of K^+ toxicity: glutamate excitotoxicity

Glutamate is a major excitatory neurotransmitter in the mammalian CNS but is also a potent neurotoxin. Glutamate activates several families of inotropic and metabotropic receptors commonly known as AMPA (e.g. GluR 1-4), kainate, NMDA (e.g. NMDAR-1 and NMDAR2A-D) and metabotropic receptors. Although all these receptor subtypes are found in neurons, astrocytes mainly express AMPA and kainate receptor subtypes (Kandel et al., 2000).

Glutamate uptake from the extracellular space is necessary for controlling excitatory postsynaptic currents as well as preventing excitotoxic neuronal cell death (Anderson and Swanson, 2000; Matute et al., 2002). Clearance of glutamate from the ECS is done by transporter mediated uptake. Glutamate transporters are expressed in astrocytes, neurons, oligodendrocytes and microglia but uptake by astrocytes is quantitatively the most important

for maintaining normal extracellular glutamate concentrations (Anderson and Swanson, 2000). In astrocytes, the glutamate transporter GLT-1 has the highest level of expression and is responsible for the clearance of extracellular glutamate, thus making it a limiting factor in glutamate neurotoxicity (Matute et al., 2002; Chen and Swanson, 2003).

Glutamate uptake requires movement against a steep concentration gradient as extracellular glutamate concentration is approximately 2μM whereas intracellular concentrations range from 1 to 10mM. This gradient is overcome by coupling the inward movement of each glutamate molecule, three Na^+ ions and one H^+ ion with the outward movement of one K^+ ion (Anderson and Swanson, 2000). The process requires energy and consumes a significant fraction of total brain ATP turnover (Sibson et al., 1998). Once taken up by astrocytes, glutamate is metabolized into glutamine or enters the TCA cycle. Glutamine synthetase (GS), a marker of astrocytes, converts glutamate into glutamine which requires ATP (Anderson and Swanson, 2000). The distribution of glial glutamate receptors and transporters parallels the location of GS (Suarez et al., 2002). One advantage of having these astrocyte-based glutamate clearance mechanisms is that it shifts energy consuming activities away from the neurons (Chen and Swanson, 2003). High extracellular K^+ can therefore increase glutamate release both through membrane depolarization of nerve terminals and/or by affecting glutamate transporters and its uptake mechanism in astrocytes (Chen and Swanson). Indeed, a knock-down of glutamate transporters produces excitotoxic neurodegeneration and an increased susceptibility to seizures (Tanaka et al., 1997; Chen and Swanson, 2003).

Astrocyte swelling has also been related to the production of glutamine. Glutamine is converted in the astrocytes from glutamate, which releases ammonia. Intracellular glutamine

accumulation is thought to underlie ammonia-induced cell swelling (Tanigami et al., 2005) which can be partially prevented via the glutamine synthetase inhibitor methionine sulfoximine (Tanigami et al., 2005).

The cellular and molecular mechanisms of glutamate excitotoxicity, including that which affects the survival of astrocytes and axons, has been extensively described in the literature (Olney and Sharpe, 1969; Choi, 1994; Senatorov et al., 2000; Sattler et al., 2001; Dodd, 2002; Matute et al., 2002). For example, excessive glutamate can induce large membrane depolarization and a collapse of Na^+ and K^+ gradients (Senatorov et al., 2000). This leads to the opening of voltage dependent Ca^{2+} channels, an enhanced release of Ca^{2+} from intracellular stores and the reverse operation of the Na^+/Ca^{2+} exchanger (Olney and Sharpe, 1969; Choi, 1994; Stys, 1998; Sattler et al., 2001; Dodd, 2002; Matute et al., 2002). Increases in intracellular Ca^{2+} may result in pathological over-activation of various enzymes leading to cell destruction. Intracellular Ca^{2+} accumulation also leads to the activation of nitric oxide synthase (NOS), calpains, endonucleases and caspase activation (Chan, 1996). Due to space limitation, these mechanisms cannot be further discussed in detail here.

1.4 Potential Mechanisms of Tissue Split

Very few reports in the literature have explicitly described the phenomenon of the tissue split in the cerebral cortical tissue although cavity formation is common in traumatically injured spinal cord (Fitch et al., 1999). Tissue specimens from rat hippocampus where cholinergic innervation from the septum was significantly removed also shows a prominent tissue split along the SGZ (Leung et al., 2003). The morphology of such a split is remarkably similar to what we found here. Clinically, however, cerebral cavity

usually results from tissue infarction although split-like tissue pathology was noticed in the DG area of post-mortem tissue obtained from patients with Alzheimer's disease (Duyckaerts et al., 1998).

Although sustained seizure activities are often associated with an increase in external K^+ concentration, autopsy results from TLE patients do not usually show a tissue split in the DG. This negative finding seems consistent with our experiments in rats, which showed that a seizure, per se, is unlikely the cause of the tissue split. For short experimental time points, our rats remained under deep anesthesia and none of the treatments led to any seizure activity or myoclonic contractions. In fact, a tissue split can be observed in 10 minutes after a K^+ injection under deep barbiturate anesthesia. When longer time points were used, the rats were allowed to regain consciousness and remained under constant supervision. Even in these longer recovery circumstances, no seizure activity was ever observed. Therefore, under our experimental conditions, an elevated extracellular K^+ but not the seizure activity appears both necessary and sufficient to produce a tissue split.

In this thesis we coined the term tissue split to emphasize the stereotypical morphological change that separates the dentate hilus from the granular cell layer. This location selectivity of the tissue split is indeed remarkable. For instance, in a number of rats we missed our injection targets (e.g. injections of K^+ solutions were made outside the hilus) but none of these cases induced a tissue split. Furthermore, despite a rather homogenous loss of astrocytes in the hilus, the split did not occur within the hilus. Similarly K^+ injections made in the cerebral cortex gave rise to a very localized tissue reaction but no tissue split was found (n=15; unpublished observations). Hence, the cellular elements and/or the structural organization of axons and astrocytes in the SGZ appear to make this region particularly

sensitive to K^+ toxicity. The mechanism of this vulnerability remains to be investigated. Interestingly, the SGZ contains polymorph progenitor cells and several types of interneurons which are selectively damaged during the very early stage of TBI (Toth et al., 1997).

Based on the experimental evidence presented in this study and those reported in the literature, we proposed that the following sequence of cellular events may be responsible for the occurrence of the tissue split.

1. Initiation stage. During which a large surge in external K^+ concentration triggers rapid swelling in astrocytes and perhaps local axons.

2. Deformation stage. During this period, severe astrocyte swelling and osmotic stress has developed in the hilus region. This creates a strong shear force across the SGZ where most thin processes from glia and neurons transverse into the GCL and are "held" by tightly packed granular neurons.

3. Split stage. In this final stage, tissue elements in the SGZ are no longer able to sustain the mechanical stress created by swelling and stretching. The further loss of astrocytes and damaged axons eventually leads to the separation of the hilus and GCL and the appearance of a tissue split between the two.

Although this hypothesis remains sketch, several lines of evidence are consistent with the overall scheme.

Firstly, as discussed above, K^+ is very potent in triggering rapid astrocyte swelling. Throughout our study, we found that GFAP positive astrocytes swell to more than twice their original size under conditions of high extracellular K^+ (Figure 3.4). Severe swelling was seen both at the somatic level and in fine processes. The onset and degree of glia swelling could be, however, underestimated in our study since many astrocytes may have already

undergone necrosis, membrane disintegration or have diminished expression of GFAP when the tissue samples were taken (see below).

Secondly, if astrocytes and other cellular elements in the hilus and SGZ swell whereas the volume of GCL neurons remains relatively unaffected, an asymmetrical shear force can develop between the hilus and GCL. Since neurons in the GCL are present as a layered structure with high packing density, the "pulling" force from the hilus will likely be imposed upon the SGZ. The unique structural relationship between the hilus and GCL neurons was also thought to be responsible for the rapid and selective injury of interneurons in the SGZ caused by skull impact during TBI (Toth et al., 1997).

The experimental evidence supporting tissue stretch and deformation remains lacking. Our laboratory has attempted to use an *in vitro* slice preparation to create a K^+-induced tissue split. However, in a thin tissue slice the cellular elements are not tightly anchored. As a result, a tissue split cannot be consistently induced even with 50 mM external K^+ (Cedrone et al., unpublished data). However, very often we observed an increase in transmission light along the SGZ after an application of a high K^+ solution. Furthermore, indirect measurement of tissue deformation was performed based on macroscopic movement of the tissue slice. It was found that in the high K^+ solution, the hippocampal DG underwent an slow upward (dorsolateral) shift from the original position which did not occur in normal perfusion medium (Chomiak and Hu, unpublished data).

Thirdly, around the tissue split zone, we found strong evidence suggesting mechanical force-related tissue damage. When examined under higher magnification, it became very obvious that the astrocyte processes were dissociated from their cell bodies which remained in the hilar region (Figure 3.5). Since these severed processes were still

intensely stained with GFAP and showed normal morphology and shape, the soma-process detachment in the astrocytes must occur quickly, possibly due to mechanical force. This assertion is consistent with our data indicating a large number of astrocytes along the tissue split region lost their membrane integrity within 30 min of high K^+ exposure. Interestingly, using PBFI, one could see certain "filaments" in the GCL. The diameters of these K^+ filaments were similar to that of the GFAP filaments observed in high extracellular K^+ concentration (Figure 3.6), suggesting glial processes themselves may also be sensitive to a high K^+ insult. It should be pointed out that high K^+ or ouabain also induced a far greater extent of cell death at a later time in the center region of the hilus. After four hours, there were approximately only 15-20 immunoreactive astrocytes left in the hilus region, accounting for a mere 17% of total astrocytes seen under control conditions (Figure 3.2 and 3.3). This "delayed" disappearance of astrocytes, however, appears different from the morphological changes observed in broken glia in the tissue split zone where a high level expression of GFAP was detected.

Lastly, glial cells play an important role in supporting the structure of the neural network (Nedergaard et al., 2003). Using neural filament staining we showed that the loss of glial support in the SGZ is associated with the appearance of axotomy in GCL neurons. Axonal injury in TBI has often been linked to mechanical impact. Permanent physical deformation can result if the force exceeds the elastic limit of the cell membrane, neurofilaments or other intraaxonal organelles (Meythaler et al., 2001). The cytoplasm can be displaced by the sustained acceleration or deceleration inertia forces that results in cytoplasmic flow causing intraaxonal damage to the neurofilament subunits and failure of the axonal cytoskeleton. This intracellular disruption may also initiate secondary biochemical

events that are calcium-dependent resulting in additional neurofilament disassembly (Meythaler et al., 2001).

The above proposed scheme of tissue split obviously needs further validation, especially at the cellular and molecular levels. For instance, although the Na-K-2Cl co-transporters and glutamate may underlie K^+-induced astrocyte swelling, we found that the tissue split in the DG was effectively blocked by K^+ channel blockers but not by a glutamate receptor antagonist. This suggests the presence of alternative mechanisms of swelling involving K^+ channels. Influx of K^+ through voltage-dependent and leak K^+ channels can take place quickly. Therefore, channel-mediated ion flux may serve as an initial trigger for tissue swelling, which exacerbates over time likely as a result of ion transporter activation and glutamate release. In intact retina, efflux of K^+ through Kv4.1 channels acts as an important mechanism in preventing astrocyte swelling (Pannicke et al., 2004; Uckermann et al., 2004). Further understanding the functional interactions between ion channels and transporters may shed important light into this matter.

1.5 Relevance to Traumatic Brain Injury

The K^+-induced tissue toxicity has not been recognized as a cellular event of significant pathological significance. Below I wish to highlight some pathological features of TBI and TLE that appear to be intimately linked to K^+ homeostasis.

1.5.1 Reactive astrocytes

The acceleration and deceleration forces associated with head injury produce stretching and shearing of neurons and blood vessels (Gaetz, 2004). The subsequent

processes, including hemotoma formation and edema, further lead ischemic and excitotoxic damage in astrocytes and neurons (Xiong et al., 1997). At a cellular level, an early primary cell death resulting from the physical impact is often followed by cascades of downstream molecular and biochemical events, which may lead to a depletion of ATP and failure in glutamate uptake (Seki et al., 1999; Brott et al., 2000; Ayata et al., 2002; Chen and Swanson, 2003). Microdialysis studies have indeed shown a six-fold increase in extracellular glutamate following fluid-percussion injury in the rat (Katayama et al., 1990).

Almost immediately following TBI, any surviving astrocytes in the affected area undergo astrogliosis (Zhao et al., 2003). Reactive astrocytes are characterized by many cellular changes including cytoplasmic enlargement, generation of long cytoplasmic processes and increased amounts of GFAP expression (Baldwin and Scheff, 1996) but more importantly, during this period they often loss their ability to buffer extracellular K^+, a phenomenon often associated with the development of tissue injury (Bordey et al., 2000; Zhao et al., 2003). In a study by Grisar et al., (1992), the activity of the Na^+,K^+-ATPase in astrocytes was found to be significantly decreased during focal epilepsy in comparison to control cells or non-epileptic areas. This impairment is associated with a decreased affinity of the pumps catalytic subunit for extracellular K^+, which is normally required for pump de-phosphorylation and Na^+ release.

Many proteins are up-regulated during astrogliosis such as copper-zinc superoxide dismutase, glutathione peroxidase and metallothionein which indicate an enhanced capacity to reduce any reactive oxygen species (ROS). The astrocytes also begin to express an inducible form of heme oxygenase, which is the first step of heme metabolism that is important in preventing heme iron participation in metal catalyzed free radical production,

particularly after an injury that liberates hemoglobin into the brain parenchyma (Chen and Swanson, 2003). Injured astrocytes also produce many cytokines such as tumor necrosis factors (TNF-α and TNF-β), interleukins (IL-1, IL-6 and IL-10), which can modulate GFAP mRNA levels, and interferons (IFN-α and IFN-β). IL-6 has been shown to protect against ischemic and excitotoxic injury and hippocampal neurons treated with TNF-α before injury are less vulnerable to substrate deprivation and excitotoxicity (Cheng et al., 1994).

1.5.2 K^+ Buffering in TBI and Epilepsy

The impairment of K^+ homeostasis takes place at two different stages of TBI: the initial large rise of external K^+ concentration and a much slower and perhaps gradual loss of K^+ buffering capacity in glia. This latter mechanism may lead to further accumulation of extracellular K^+, contributing to seizure (D'Ambrosio et al., 1999). MacFarlane and Sontheimer (1997) proposed that injured astrocytes show an up-regulation in outwardly rectifying K^+ currents and a down-regulation in inwardly rectifying K_{IR} currents. The K_{IR} channels can also be inhibited by the drop in extracellular Na^+ (D'Ambrosio et al., 1999). Bordey and Sontheimer (1998) found that cells from patients suffering from epilepsy show a 7-fold increase in Na^+ channel expression with a significant reduction in the expression of inwardly rectifying K^+ channels, which are the dominant form of K^+ conductance in adult CNS astrocytes.

In a series of *in vitro* electrophysiological studies conducted in our laboratory, it was found that astrocytes in the SGZ responded to high extracellular K^+ (10-14 mM) with a up to a 70% reduction of membrane potassium conductances (Hu et al., 2004). The macroscopic current of these voltage-clamped cells showed both reduced outward and inward

rectifications, which persisted even after high external K^+ concentration was returned to 3 mM. Similar recordings from neighboring GCL neurons showed an opposite trend of K^+ modulation. Although the exact cause of this K^+-mediated closure of membrane conduction is unknown, the ion channel-based K^+ homeostasis mechanism in astrocytes seemed quickly paralyzed by high potassium itself.

1.5.3 Astrocyte death and TBI

Early impairment of astrocyte function after TBI may compromise the maintenance of homeostasis in the extracellular environment and would disrupt neuronal-glial interactions. Zhao et al., (2003) investigated the time course of damage and loss of astrocytes after FPI in rats. They found that astrocytes in the ipsilateral region revealed a loss of GFAP immunostaining as early as 30 minutes post-FPI. This suggests that following TBI, astrocytes are rapidly damaged and lost in vulnerable brain regions and may precede neuronal degeneration. Furthermore, they found that the loss of immunoreactivity of GFAP is not a result of a loss of antigen sites but the damage or loss of astrocytes themselves. Firstly, GFAP loss is selective and occurs only in the hippocampal brain region that also has neuronal degeneration and loss. Secondly, in studies where immunohistochemistry was performed with two astrocyte markers (both GFAP and GS), there was a loss of both indicating the signal loss is not selective to GFAP antigen. Rather it can be readily explained based on the disassembly of intermediate filaments (Zhao et al., 2003). The finding of an early astrocyte injury by Zhao et al. is consistent with the feature of K^+-induced hippocampal lesion described in this thesis.

1.5.4 Axonal Disconnections

Axonal damage is the predominant form of tissue abnormality found in 40-50% of TBI patients (Meythaler et al., 2001). Disruption of the neurofilament subunits of the axonal cytoskeleton may result from sustained acceleration and deceleration forces imposed to the skull. In the study by Singleton et al. (2002), it was observed that at 30 minutes post-injury (using a FPI injury model), axonal swelling occurred in the thalamus, neocortex and hippocampus. After two hours, they found that only a few of the injured axons were still continuous with their downstream segments and at the 4-6 hour time point, there was no continuity seen between the cell bodies and their distal axonal segments. Interestingly, although the axonal damage was as close as 20-50μm from the soma of the neuron, this axotomy did not result in immediate cell death. It is noteworthy that in our model, the tissue split induced axotomy but not neuronal loss. In fact, staining granular neurons with NeuN showed no cell loss within 72 hours immediately following a tissue split (Cedrone et al., 2005). When ethidium bromide was injected into the hippocampus along with a solution of 5mM K^+, there was cell death present (Figure 3.1). However, the region of cell death strongly overlapped with GFAP staining along the tissue split border but not GCL.

Axonal injury was originally thought to occur immediately after TBI due to tearing however, it is now known that this tearing rarely occurs (Povlishock and Jenkins, 1995). After TBI, there is often a depolarization of the cell followed by a focal loss of axonal transport due to a disruption of the cellular organelles (Povlishock and Jenkins, 1995). This direct mechanical displacement of the cytoskeleton and cytoplasm leads to further neuronal cell injury and axonotmesis. In this context, it would be interesting to further investigate whether K^+-induced axonal transport failure as described by Humari et al., (1999) plays a

role in axonal disconnections associated with TBI.

Although axotomy can take place without a loss of the cell somata, gradual cell death and loss of neurons are inevitable over longer time period. This degenerative process of TBI may involve depletion of ATP, intracellular calcium overload, oxidative stress, glutamate excitotoxicity, and an abnormal activation of NMDA receptors (Philips et al., 1998) together with increased calpain and caspase-3 activities (Buki et al., 2000). During the several hours following TBI, there is also compaction of the neurofilaments and the collapse of their sidearms as well as a loss of axonal microtubules. Therefore, even in cells which may have been able to recover from the original insult, these secondary factors may lead to delayed cell loss as a result of necrosis and/or apoptosis (Meythaler et al., 2001). In supporting to this postulation, our laboratory recently found that the tissue split does lead to significant loss of granular neurons 3-5 days after the initial insult, especially around the K^+ injection sites (Cedrone et al., 2005). Long term memory deficits characteristic of partial hippocampal damage and those induced by TBI (Scheff et al., 1997) is also evident in these rats, suggesting acute axotomy and tissue split may lead to long-term impairment of hippocampal function. Interestingly, the tissue split was completely "sealed up" during this time period (Cedrone et al., 2005).

1.6 Conclusions and Future Directions

Moderate to high levels of extracellular K^+ concentration is traditionally thought a benign tissue response. This thesis work demonstrates for the first time that excess extracellular K^+ can actually cause acute brain damage leading to long term neurodegeneration. We propose that this situation arises mainly due to the fact that

astrocytes within the hippocampal hilus become swollen and incapable of buffering K^+ and maintaining the structural integrity of the surrounding tissue. These cellular events lead to glial cell severance and death and further results in a tissue split along the SGZ. It would be of a great value if a similar pathological situation can be recreated in an *in vitro* model, allowing studies to be conducted with a greater control of the cellular milieu.

References:

Adelman W.J. and R. Fitzhugh. (1975) Solutions of the Hodgkin-Huxley equations modified for potassium accumulation in periaxonal spaces. *Fedn. Proc.* **34**: 1322-29.

Amédée T., Robert A. and J.A. Coles. (1997) Potassium homeostasis and glial energy metabolism. *Glia* **21**:46-55.

Anderova M., Kubinova S., Mazel T., Chvatal A., Eliasson C, Pekny M and E. Sykova. (2001) Effect of elevated K^+, hypotonic stress, and cortical spreading depression on astrocyte swelling in GFAP-deficient mice. *Glia.* **35**(3):189-203.

Anderson C.M. and R.A. Swanson. (2000) Astrocyte glutamate transport: Review of properties, regulation, and physiological functions. *Glia.* **32**:1-14.

Annegers J.F. and S.P. Coan. (2000) The risks of epilepsy after traumatic brain injury. *Seizure.* **9**: 453-57.

Ayata C. and A.H Ropper (2002) Ischaemic brain oedema. *J Clin Neurosci* **9**:113-24.

Baldwin S.A. and S.W. Scheff. (1996) Intermediate filament change in astrocytes following mild cortical contusion. *Glia.* **16**:266-75.

Balestrino M., Aitken P.G. and G.G. Somjen. (1986) The effects of moderate changes of extracellular potassium and calcium on synaptic and neuronal function in the CA1 region of the hippocampal slices. *Brain Res* **377**:229-39.

Balestrino M., Young J. and P. Aitken. (1999) Block of Na^+,K^+-ATPase with ouabain induces spreading depression-like depolarization in hippocampal slices. *Brain Res.* **838**: 37-44.

Ballanyi K., Grafe P. and G. ten Bruggencate. (1987) Ion activities and potassium uptake mechanisms of glial cells in guinea-pig olfactory cortex slices. *J. Physiol.* **382**: 159-74.

Bass, N.H., Hess, H.H., Pope, A. and C. Thalheimer. (1971) Quantitative cytoarchitectonic distribution of neurons, glia and DNA in rat cerebral cortex. *J. Comp. Neurol.* **143**: 481-90.

Bondarenko A. and M. Chesler. (2001) Rapid astrocyte death induced by transient hypoxia,

acidosis, and extracellular ion shifts. *Glia.* **34**:134-42.

Bondarenko A., Svichar N. and M. Chesler. (2004) Role of Na^+-H^+ and Na^+-Ca^{2+} exchange in hypoxia-related acute astrocyte death. *Glia.* **49**:143-52.

Bordey A. and H. Sontheimer. (1998) Properties of human glial cells associated with epileptic seizure foci. *Epilepsy Research* **32**: 286-303.

Bordey A., Lyons S.A., Hablitz J.J. and H. Sontheimer. (2000) Electrophysiological characteristics of reactive astrocytes in experimental cortical dysplasia. *J Neurophysiology* **85**(4): 1719-31.

Brott T. and J. Bogousslavsky (2002) Treatment of acute ischemic stroke. *N Engl J Med* **343**:710-22.

Bruton C. (1988) The neuropathology of temporal lobe epilepsy. New York: Oxford UP.

Buckmaster P.S., Yamawaki R. and G.F. Zhang. (2002) Axon arbors and synaptic connections of a vulnerable population of interneurons in the dentate gyrus in vivo. *J. Comp. Neurol.* **445**:360-73.

Büki A., Okonkwo D.O., Wang K.K. and J.T. Povlishock. (2000) Cytochrome c release and caspase activation in traumatic axonal injury. *J Neurosci.* **20**(8): 2825-34.

Büki A., Farkas O., Doczi T. and J.T. Povlishock. (2003) Preinjury administration of the calpain inhibitor MDL-28170 attenuates traumatically induced axonal injury. *J Neurotrauma* **20**(3): 261-8.

Bushong E.A., Martone, M.E., Jones, Y.Z. and M.H. Ellisman. (2002) Protoplasmic astrocytes in CA1 stratum radiatum occupy separate anatomical domains. *J. Neurosci.* **22**: 183-92.

Buzsaki G., Leung L.W. and C.H. Vanderwolf (1983) Cellular basis of hippocampal EEG in the behaving rat. Brain Res 287: 139-171.

Cedone C., Dyke R.H. and B. Hu. (2005) The role of elevated extracellular potassium in hippocampal dentate cell death and memory deficits. *Society for Neurosciences Abstract.*

Chan P.H. (1996) Role of oxidants in ischemic brain damage. *Stroke* **27**:1124-9.

Chen Y. and R.A. Swanson. (2003) Astrocytes and Brain Injury. *J. Cereb. Blood Flow.* **23**:137-49.

Cheng B., Christakos S. and M.P. Mattson. (1994) Tumor necrosis factors protect neurons against metabolic-excitotoxic insults and promote maintenance of calcium homeostasis. *Neuron.* **12**: 139-53.

Choi D.W. (1994) Glutamate receptors and the induction of excitotoxic neuronal death. *Prog Brain Res* **100**:47-51.

Coulter D.A., Rafiq A., Shumate M., Gong Q.Z., DeLorenzo R.J. and Lyeth B.G. (1996) Brain injury-induced enhanced limbic dpileptogenesis:anatomical and physiological parallels to an animal model of temporal lobe epilepsy. *Epilepsy Res.* **26**: 81-91.

D'Ambrosio R., Mans D.O., Grady M.S., Winn H.R. and D. Janigro. (1998) Selective loss of hippocampal long-term potentiation, but not depression, following fluid percussion injury. *Brain Res.* **786**: 64-79.

D'Ambrosio R., Wenzel J., Schwartzkroin P.A., McKhann G.M. and D. Janigro. (1998) Functional specialization and topographic segregation of hippocampal astrocytes. *J. Neurosci.* **18**(12): 4425-38.

D'Ambrosio R., Maris D.O., Grade M.S., Winn H.R. and D. Janigro. (1999) Imparied K+ homeostasis and altered electrophysiological properties of post-traumatic hippocampal glia. *J. Neurosci.* **19**(18): 8152-62.

Di X., Lyeth B.G., Hamm R.J. and M.R. Bullock. (1996) Voltage-dependent Na+/K+ ion channel blockade fails to ameliorate behavioral deficits after traumatic brain injury in the rat. *J. Neurotrauma* **13**(9): 497-504.

Dihné M., Block F., Korr H. and R. Töpper. (2001) Time course of glial proliferation and glial apoptosis following excitotoxic CNS injury. *Brain Res.* **902**:178-89.

Dodd P.R. (2002) Excited to death: Different ways to lose your neurons. *Biogerontology* **3**:51-6.

Doherty J. and R. Dingledine. (2001) Reduced excitatory drive onto interneurons in the dentate gyrus after status epilepticus. *J Neurosci.* 21(6): 2048-57.

Duyckaerts C., Colle M.A., Seilhean D. and J.J. Hauw. (1998) Laminar spongiosis of the dentate gyrus: a sign of disconnection, present in cases of severe Alzheimer's disease. *Acta Neuropathol (Berl).* **95**(4): 413-20.

Eddleston M., de la Torre J.C., Campbell I.L. and M.B. Oldstone (1996) The M22 antibody

identifies highly activated reactive astrocytes responding to central nervous system disease. *Acta Neuropathol.* **91**: 298-308.

Eng L.F., Ferstl B. and J.J. Vanderhaeghen. (1970) A study of proteins in old multiple sclerosis plaques. *Trans. Am. Soc. Neurochem.* **1**: 42.

Eng L.F. and Y.L. Lee. (1995) Intermediate filaments in astrocytes. In Neuroglial cells (Ransom BR, Kettenmann H, ed), New York: Oxford University Press. Pp 650-667.

Eng L.F., Girnikar R.S., and Yuen L. Lee. (2000) Glial Fibrillary Acidic Protein: GFAP-Thirty-One Years (1969-2000). *Neurochemical Research* **25** (9/10): 1439-51.

Erecinska M. and I.A. Silver. (1994) Ions and energy in mammalian brain. *Prog Neurobiol.* **43**: 37-71.

Esselman P.C., Dikmen S.S., Bell K. and N.R. Temkin. (2004) Access to inpatient rehabilitation after violence-related traumatic brain injury. *Arch. Phys. Med. Rehabil.* **85**:1445-1449.

Fields R.D., and B. Stevens-Graham. (2002) New Insights into Neuron-Glia Communication. *Science* **298** (5593): 556-62.

Fisher R.S., Pedley T.A., Moody W.J. and D.A. Prince. (1976) The role of extracellular potassium in hippocampal epilepsy. *Arch Neurol.* **33**(2): 76-83.

Fitch M.T., Doller C., Combs C.K., Landreth G.E. and J. Silver. (1999) Cellular and molecular mechanism of glial scarring and progressive cavitation: In vivo and In vitro analysis of inflammation-induced secondary injury after CNS trauma. *J. Neuroscience.* **19**(19): 8182-98.

Gaetz M. (2004) The neurophysiology of brain injury. *Clin. Neurophysiol.* **115**:256-58.

Geck P., Pietrzyk C., Burckhardt B-C., Pfeiffer B. and E. Heinz. (1980) Electrically silent co-transport of Na^+, K^+ and Cl^- in Ehrlich cells. *Biochim Biophys Acta* **600**: 432-47.

Geering K., Beggah A., Good P., Girardet S., Roy S., Schaer D. and P. Jaunin. (1996) Oligomerization and maturation of Na,K-ATPase: functional interaction of the cytoplasmic NH2 terminus of the beta subunit with the alpha subunit. *J. Cell Biol.* **133**(6): 1193-201.

Glynn I.M. and S.J. Karlish. (1990) Occluded cations in active transport. *Ann. Rev. Biochem.* **59**: 171-205.

Gomi H., Yokoyama T., Fujimoto K., Ikeda T., Katoh A., Itoh T., and S. Itohara. (1995) Miceo devoid of the glial fibrillary acidic protein develop normally and are susceptible to scrapie prions. *Neuron.* **14**(1):29-41.

Golarai G., Greenwood A.C., Feeney D.M. and J.A. Connor. (2001) Physiological and structural evidence for hippocampal involvement in persistent seizure susceptibility after traumatic brain injury. *J. Neurosci.* **21**(21): 8523-37.

Hertz L. (1965) Possible role of neuroglia: a potassium-mediated neuronal-neuroglial-neuronal impulse transmission system. *Nature.* **206**:1091-94.

Hertz L., Peng L. and Lai J. (1998) Functional Studies in Cultured Astrocytes. *Methods* **16**: 293-310.

Hiruma H., Nishida S., Katakura T., Kusakabe T., Takenaka T. and T. Kawakami. (1999) Extracellular potassium rapidly inhibits axonal transport of particles in cultured mouse dorsal root ganglion neurites. *J Neurobiology* **38**(2): 225-33.

Holscher C. (2003) Time, space and hippocampal functions. *Rev. Neurosci.* **14**(3): 253-84.

Horner P. and T. Palmer. (2003) New roles for astrocytes: the nightlife of an 'astrocyte'. La vida loca! *Trends Neurosci.* **26**(11): 597-603.

Hu B., Li Z., Basile C., Cedrone C. and A. Omar. Potassium ions cause rapid tissue injury in rat dentate hilus. Society for Neuroscience Annual Meeting. November 2004. San Diego, California, USA.

Ingvar M., Schmidt-Kastner R. and D. Meller. (1994) Immunohistochemical markers for neurons and astrocytes show pan-necrosis following infusion of high-dose NMDA into rat cortex. *Exp Neurol.* **128**:249-59.

Kandel E.R., Schwartz J.H. and T.M. Jessell. (2000) Principles of Neural Science. 4th Ed. New York: McGraw-Hill Publishing.

Katayama Y., Becker D.P., Tamura T. and D.A. Hovda. (1990) Massive increases in extracellular potassium and the indiscriminate release of glutamate following concussive brain injury. *J. Neurosurg.* **73**(6): 889-900.

Kawamata T., Katayama Y., Hovda D.A., Yoshino A. and D.P. Becker. (1995) Lactate accumulation following concussive brain injury: the role of ionic fluxes induced by excitatory amino acids. *Brain Res.* **674**(2):196-204.

Kettenmann H., Banati R. and W. Walz. (1993) Electrophysiological behavior of microglia. *Glia.* 7 :93-101.

Kreisman N.R. and M.L. Smith. (1993) Potassium-induced changes in excitability in the hippocampal CA1 region of immature and adult rats. *Dev. Brain Res.* **76**:67-73.

Kullmann D.M. and A. Semyanov. (2002) Glutamatergic modulation of GABAergic signaling among hippocampal interneurons: novel mechanisms regulating hippocampal excitability. *Epilipsia.* **43**(Suppl. 5): 174-78.

Lee T.S., Eid T., Mane S., Kim J.H., Spencer D.D., Ottersen O.P. and N.C. deLanerolle. (2004) Aquaporin-4 is increased in the sclerotic hippocampus in human temporal lobe epilepsy. *Acta Neuropathol.* **108**(6): 493-502.

Lees G.J. and W. Leong. (1994) Brain lesions induced by specific and non-specific inhibitors of sodium-potassium ATPase. *Brain Res.* **649**: 225-33.

Leis J.A., Bekar L.K. and W. Walz. (2005) Potassium homeostasis in the ischemic brain. Glia. 50(4): 407-16.

Lemas M.V., Hamrick M., Takeyasu K. and D.M. Fambrough. (1994) 26 amino acids of an extracellular domain of the Na,K-ATPase alpha-subunit are sufficient for assembly with the Na,K-ATPase beta-subunit. *J. Biol. Chem.* **269**(11): 8255-9.

Leung L.S., Shen B., Rajakumar N. and J. Ma. (2003) Cholinergic activity enhances hippocampal long-term potentiation in CA1 during walking rats. *J. Neurosci.* **23**(28): 9297-304.

Lewén A., Fredriksson A., Li G.L., Olsson Y. and L Hillered. (1999) Behavioral and morphological outcomes of mild cortical contusion trauma of the rat brain: influence of NMDA-receptor blockade. *Acta Neurochir.* **141**:193-202.

Li S. and P.K. Stys. (2001) Na^+,K^+-ATPase inhibition and depolarization induce glutamate release via reverse Na^+-dependent transport in spinal cord white matter. *Neuroscience.* **107**: 675-83.

Liedtke W., Edelmann W., Biere P.L., Chiu F.C., Cowan N.J., Kucherlapati R., and C.S. Raine. (1996) GFAP is necessary for the integrity of CNS white matter architecture and long-term maintenance of myelination. *Neuron* **17**(4): 607-15.

Lingrel J.B., Van Huysse J., O'Brien W., Jewell-Motz E., Askew R. and P. Schultheis.

(1994) Structure function studies of the Na,K-ATPase. *Kidney Int. Suppl.* 44: S32-9.

Lowenstein D.H., Thomas M.J., Smith D.H. and T.K. McIntosh. (1992) Selective vulnerability of dentate hilar neurons following traumatic brain injury: a potential mechanical link between head trauma and disorders of the hippocampus. *J. Neurosci.* **12**: 4846-53.

Lucas D.R. and J.P. Newhouse. (1957) The toxic effect of sodium L-glutamate on the inner layers of the retina. *Arch. Ophthalmol.* **58**: 193-201.

Ludwin S.K., Kosek J.C. and L.F. Eng. (1976) The topographical distribution of S-100 and GFAP in the adult rat brain: an immunohistochemical study using horseradish peroxidase-labelled antibodies. *J. Comp. Neurol.* **165**: 197-207.

MacFarlane S.N. and H. Sontheimer. (1997) Electrophysiological changes that accompany reactive gliosis *in vitro*. *J. Neurosci.* **17**(19): 7316-29.

Malhotra S.K. and T.K Shnitka (1994) *Biomed. Lett.* **49**: 273-302.

Manley G.T., Fujimura M., Ma T., Noshita N., Filiz F., Bollen A.W., Chan P. and A.S. Verkman. (2000) Aquaporin-4 deletion in mice reduces brain edema after acute water intoxication and ischemic stroke. *Nat Med.* **6**(2): 159-63.

Margerison J.H. and J.A. Corsellis (1966) Epilepsy and the temporal lobes. A clinical, electroencephalographic and neuropathological study of the brain in epilepsy, with particular reference to the temporal lobes. *Brain* **89**: 499-530.

Matthews, J.B. (2002) Molecular regulation of Na^+-K^+-$2Cl^-$ cotransporter (NKCC1) and epithelial chloride secretion. *World J. Surg.* **26**: 826-30.

Matute C., Alberdi E., Ibarretxe G. and M.V. Sánchez-Gómez. (2002) Excitotoxicity is glial cells. *Eur. J. Pharm.* **447**: 239-46.

Maxwell W.L., Povlishock J.T. and D.L. Graham. (1997) A mechanistic analysis of nondisruptive axonal injury: a review. *J Neurotrauma* **14**(7): 419-40.

McCall, M.A., Gregg R.G., Behringer R.R., Brenner M., Delaney C.L., Galbreath E.J., Zhang C.L., Pearce R.A., Chiu S.Y. and A. Messing. (1996) Targeted deletion in astrocye intermediate filament (GFAP) alters neuronal physiology. *PNAS* **93**(13): 6361-6.

McGrail K.M., Phillips J.M. and K.J. Sweadner. (1991) Immunofluorescent localization of

three Na,K-ATPase isozymes in the rat central nervous system: both neurons and glia can express more than one Na,K-ATPase. *J. Neurosci* **12**(2): 381-91.

Messing A., Head M.W., Galles K., Galbreath E.J., Goldman J.E. and M. Brenner. (1998) Fatal encephalopathy with astrocyte inclusions in GFAP transgenic mice. *Am J Pathol* **152**:391-98.

Messing A., and M. Brenner. (2003) GFAP: Functional Implications Gleaned From Studies of Genetically Engineered Mice. *Glia* **43**: 87-90.

Meythaler J.M., Peduzzi J.D., Eleftheriou E. and T.A. Novack. (2001) Current Concepts: Diffuse axonal injury-associated traumatic brain injury. *Arch Phys Med Rehabil* **82**: 1461-71.

Muller M. and G.G. Somjen. (2000) Na+ and K+ concentrations, extra- and intracellular voltages, and the effect of TTX in hypoxic rat hippocampal slices. *J. Neurophysiol.* **83**(2): 735-45.

Nagelhus E.A., Veruki M.L., Torp R., Haug R.M., Laake J.H., Nielsen S., Agre P. and O.P. Ottersen. (1998) Aquaproin-4 water channel protein in the rat retina and optic nerve: polarized expression in Muller cells and fibrous astrocytes. *J. Neurosci.* **18**: 2506-19.

Nawashiro H., Brenner M., Fukui S., Shima K. and J.M. Hallenbeck. (2000) High susceptibility to cerebral ischemia in GFAP-null mice. *J Cereb Blood Fow Metab* **20**:1040-44.

Nedergaard M., Ransom B., and S. Goldman. (2003) New roles for *astrocytes*: Redefining the functional architecture of the brain. *Trends in Neuroscience* **26**(10):523-30.

O'Brien W.J., Lingrel J.B. and E.T. Wallick. (1994) Ouabain binding kinetics of rats alpha two and alpha three isoforms of the sodium-potassium adenosine triphosphate. *Arch Biochem Biophys.* **310**(1):32-9.

Olney J.W. and L.G. Sharpe. (1969) Brain lesions in an infant rhesus monkey treated with monosodium glutamate. *Science.* **166**: 386-88.

Omar A.I., Senatorov V.V. and B. Hu. (2001) Sodium-potassium adenosine triphosphatase inhibition enhances membrane accumulation of DiI in rat hippocampus in vivo. *Neuroscience* **102**, 353-9.

Omar A.I., Senatorov V.V. and B. Hu. (2000) Ethidium bromide staining reveals rapid cell dispersion in the rat dentate gyrus following ouabain-induced injury. *Neuroscience* **95**, 73-80.

Omar, A.I. Ph.D. (2002) Tissue injury and remodeling in rat hippocampal dentate gyrus following Na^+-K^+-ATPase inhibition. University of Ottawa; PhD Thesis.

Orkand R.K., Nicholls J.G and S.W. Kuffler. (1966) The effect of nerve impulses on the membrane potential of glial cells in the central nervous system of amphibia. *J. Neurophysiol.* **29**: 788-806.

Pannicke T., Iandiev I., Uckermann O., Biedermann B., Kutzera F., Wiedemann P., Wolburg H., Reichenbach A. and A. Bringmann. (2004) A potassium channel-linked mechanism of glial cell swelling in the postischemic retina. *Mol Cell Neurosci.* **26**(4): 493-502.

Payne J.A., Rivera C., Voipio J. and K. Kaila. (2003) Cation-chloride co-transporters in neuronal communication, development and trauma. *Trends in Neurosci.* **26A**: 199-206.

Paxinos G. and C. Watson. (1998) The rat brain in stereotaxic coordinates. 4th Ed. *Academic Press*, London.

Pekny M., Leveen P., Pekna M., Eliasson C., Berthold CH., Westermark B., and C. Betsholtz. (1995) Mice lacking glial fibrillary acidic protein display astrocytes devoid of intermediate filaments but develop and reproduce normally. *EMBO J.* **14**(8): 1590-8.

Pekny M., Stanness K.A., Eliasson C., Betsholtz C. and D. Janigro. (1998) Impaired induction of blood-brain barrier properties in aortic endothelial cells by astrocytes from GFAP-deficient mice. *Glia* **22**: 390-400.

Pfrieger F. and B. Barres. (1997) Synaptic efficacy enhanced by glial cells in vitro. *Science.* **277**(5332):1684-7.

Povlishock J.T. and L.W. Jenkins. (1995) Are the pathobioogical changes evoked by traumatic brain injury immediate and irreversible? *Brain Pathol.* **5**(4): 415-26.

Privat, A., Gimenez-Ribotta, M. and J-C. Ridet. (1995) Morphology of astrocytes. In: *Neuroglia* (Ransom BR, Kettenmann H eds), New York: Oxford University Press, pp

3-22.

Reinert M., Khaldi A., Zauner A., Doppenberg E., Choi S. and R. Bullock. (2000) High level of extracellular potassium and its correlates after severe head injury relationship to high intracranial pressure. *J Neurosurg.* **93**(5): 800-7.

Ridet J., Malhotra S., Privat A., and F. Gage. (1997) Reactive astrocytes: cellular and molecular cues to biological function. *Trends Neurosci.* **20**:570-77.

Ross S.T. and I. Soltesz. (2000) Selective Depolarization of Interneurons in the Early Posttraumatic Dentate Gyrus: Involvement of the Na+/K+-ATPase. *J. Neurophys.* **83**(5):2916-30.

Russell J.M. (2000) Sodium-Potassium-Chloride Cotransport. *Phys Rev.* **80**(1): 211-76.

Santhakumar V., Bender R., Frotscher M., Ross S.T., Hollrigel G.S., Toth Z. and I. Soltesz. (2000) Granule cell hyperexcitability in the early post-traumatic rat dentate gyrus: the 'irritable mossy cell' hypothesis. *J. Physiol.* **524**(1): 117-34.

Santhakumar V., Ratzliff A.D., Jeng J., Toth Z. and I. Soltesz. (2001) Long-term hyperexcitability in the hippocampus after experimental head trauma. *Ann Neurol.* **50**: 708-17.

Sattler R. and M. Tymianski (2001) Molecular mechanisms of glutamate receptor-mediated excitotoxic neuronal cell death. *Mol Neurobiol* **24**:107-29.

Scheff S.W., Baldwin S.A., Brown R.W. and P.J. Kraemer. (1997) Morris water maze deficits in rats following traumatic brain injury: lateral controlled cortical impact. *J. Neurotrauma.* **14**(9): 615-27.

Scheiner-Bobis, G. (2002) The sodium pump. Its molecular properties and mechanisms of ion transport. *Eur. J. Biochem.* **269**(10): 2424-33.

Schwarcz R. and M.P. Witter. (2002) Memory impairment in temporal lobe epilepsy: the role of entorhinal lesions. *Epilepsy Res.* **50**(1-2): 161-77.

Scoville W.B. and B. Milner. (1957) Loss of recent memory after bilateral hippocampal lesions. *J. Neurochem.* **20**(1): 11-21.

Senatorov V.V., Mooney D. and B. Hu. (1997) The electrogenic effects of Na+K+-ATPase in rat auditory thalamus. *J Physiol.* 502 Pt 2:375-85.

Senatorov V.V., Stys P.K. and B. Hu. (2000) Regulation of the Na,K-ATPase by persistent

sodium accumulation in adult rat thalamic neurons. *J Physiol.* 525 Pt 2:343-53.

Sibson N.R., Dhankhar A., Mason G.F., Rothman D.L., Behar K.L. and R.G. Shulman. (1998) Stoichiometric coupling of brain glucose metabolism and glutamatergic neuronal activity. *Proc Natl Acad Sci.* **95**:316-21.

Singleton R.H., Zhu J., Stone J.R. and J.T. Povlishock. (2002) Traumatically induced axotomy adjacent to the soma does not result in acute neuronal death. *J. Neurosci.* **22**(3):791-802.

Small S.A. (2002) The longitudinal axis of the hippocampal formation: its anatomy, circuitry, and role in cognitive function. *Rev. Neurosci.* **13**(2): 183-94.

Statistics Canada (1996) National Population Health Survey. Ottawa, Statistics Canada.

Stone J.R., Walker S.A. and J.T. Povlishock. (1999) The visualization of a new class of traumatically injured axons through the use of a modified method of microwave antigen retrieval. *Acta Neuropathol* **97**: 335-45.

Stys P.K. (1998) Anoxic and ischemic injury of myelinated axons in CNS white matter: from mechanistic concepts to therapeutics. *J Cereb Blood Flow Metab* **18**(1):2-25.

Su G., Kintner D.B., Flagella M., Shull G.E. and D. Sun. (2002) Astrocytes from Na+-K+-Cl- cotransporter-null mice exhibit absence of swelling and decrease in EAA release. *Am J Physiol Cell Physiol.* **282**:1147-60.

Takenaka T. and T. Kawakami. (1996) Signal transduction mechanism responsible for changes in axoplasmic transport caused by neurotransmitters. *Neurochem Res.* **21**(5): 553-6.

Tanaka H., Katoh A., Oguro K., Shimazaki K., Gomi H., Itohara S., Masuzawa T. and Kawai N. (2002) Disturbance of Hippocampal Long-Term Potentiation After Transient Ischemia in GFAP Deficient Mice. *Journal of Neuroscience Research* **67**: 11-20.

Tanigami H., Revel A., Martin L.J., Chen T.Y., Brusilow S.W., Traystman R.J. and R.C. Koehler. (2005) Effect on glutamine synthetase inhibition on astrocyte swelling and altered astroglial protein expression during hyperammonemia in rats. *Neuroscience* **131**(2): 437-49.

Tatzelt J., Maeda N., Pekny M., Yang S., Betsholtz C., Eliasson C., Cayetano J., Camerino

A., DeArmond S., and S. Prusiner. (1996) Scrapie in mice deficient in apolipoprotein E or glial fibrillary acidic protein. *Neurology.* **47**(2):449-53.

Toth Z., Hollrigel G.S., Gorcs T. and I. Soltesz. (1997) Instantaneous perturbation of dentate interneuronal networks by a pressure wave-transient delivered to the neocortex. *J. Neurosci.* **17**(21): 8106-17.

Uckermann O., Vargova L., Ulbricht E., Klaus C., Weick M., Rillich K., Wiedemann P., Reichenbach A., Sykova E. and A. Bringmann. (2004) Glutamate-evoked alterations of glial and neuronal cell morphology in the guinea pig retina. *J. Neurosci.* **24**(45): 10149-58.

Ullian E., Sapperstein S., Christopherson K. and B. Barres. (2001) Control of synapse number by glia. *Science.* **291**(5504):569-70.

Venero J.L., Vizuete M.L., Machado A. and J. Cano. (2001) Aquaporins in the central nervous system. *Prog Neurobiol.* **63**(3): 321-36.

Vinogradova O.S. (2001) Hippocampus as comparator: role of the two input and two output systems of the hippocampus in selection and registration of information. *Hippocampus* **11**(5): 578-98.

Walz W. and W.A. Wuttke. (1999) Independent Mechanisms of Potassium Clearance by Astrocytes in Gliotic Tissue. *J. Neuroscience Research.* **56**: 595-603.

Walz W. (2000) Role of astrocytes in the clearance of excess extracellular potassium. *Neurochem. Int.* **36**: 291-300.

Wheal H.V., Bernard C., Chad J.E. and R.C. Cannon. (1998) Pro-epileptic changes in synaptic function can be accompanied by pro-epileptic hanges in neuronal excitability. *Trends Neurosci.* **21**: 167-74.

Xiong Z. and J.L. Stringer. (1999) Astrocytic regulation of the recovery of extracellular potassium after seizures *in vivo*. *Eur J Neurosci.* **11**: 1677-84.

Zhao X., Ahram A., Berman R.F., Muizelaar J.P. and B.G. Lyeth. (2003) Early loss of astrocytes after experimental traumatic brain injury. *Glia.* **44**:140-52.